

# Bridging Theory with Experiment: A Benchmark Study of Thermally Averaged Structural and Effective Spectroscopic Parameters of the Water Molecule<sup>†</sup>

Gábor Czakó,<sup>‡</sup> Edit Mátyus, and Attila G. Császár\*

Laboratory of Molecular Spectroscopy, Institute of Chemistry, Eötvös University, H-1518 Budapest 112, P.O. Box 32, Hungary

Received: March 25, 2009; Revised Manuscript Received: July 1, 2009

Extending our previous study on the equilibrium structures of the major isotopologues of the water molecule (Császár et al. *J. Chem. Phys.* **2005**, *122*, 214305), temperature-dependent averaged structural parameters (for example,  $r_g$ - and  $r_a$ -type distances, their related root-mean-square amplitudes, and moments corresponding to the probability distribution functions of interatomic distances), effective rotational constants, and low-order vibration–rotation interaction constants have been determined for two major symmetric isotopologues of water,  $\text{H}_2^{16}\text{O}$  and  $\text{D}_2^{16}\text{O}$ . The nuclear motion treatments employed full quantum mechanical variational procedures which utilized the accurate adiabatic semiglobal PESs of water isotopologues named CVRQD (Barletta et al. *J. Chem. Phys.* **2006**, *125*, 204307). The temperature-dependent molecular structural parameters are based on expectation value computations and Boltzmann averaging in the temperature range 0–1500 K. The precise computed average internuclear, inverse internuclear, rms amplitude, and anharmonicity parameters could support a future gas electron diffraction (GED) investigation, though water isotopologues are far from being ideal species for GED analyses. Using a clearly defined and general formalism applicable to molecules of any size, we have evaluated vibrationally averaged effective rotational constants as expectation values using inertia tensor formulas in the Eckart frame for vibrational states of  $\text{H}_2^{16}\text{O}$  and  $\text{D}_2^{16}\text{O}$ . While such variationally determined rotational constants do not correspond strictly to constants resulting from fits performed by spectroscopists, the expected good agreement is found for the *A* and *B* rotational constants for both isotopologues. Low-order vibration–rotation interaction constants, the so-called  $\alpha$ - and  $\gamma$ -constants, have also been determined from the computed rotational constants; the latter were derived for the first time.

## 1. Introduction

Since the advent of quantum mechanics, perturbative techniques have been playing a special and almost unique role in the development of molecular structure determination and in theoretical molecular spectroscopy, including the interpretation of the complex rotational–vibrational spectra of semirigid molecules. Although perturbation theory (PT) can be used to different orders,<sup>1</sup> traditional applications of PT in these areas have been restricted to first and second order.

Vibrational perturbation theory carried out to second-order (VPT2)<sup>2–9</sup> is still fundamental to the everyday practice of experimental and theoretical high-resolution spectroscopists, especially when dealing with molecules having more than about four-six atoms. The formulas derived within VPT are usually rather complex and some of them are somewhat involved to determine. Nevertheless, once perturbative expressions for the so-called spectroscopic molecular constants are derived and programmed, their use requires no significant computational effort.<sup>6,7</sup> This and their apparent precision contributed considerably to their widespread application. Despite the usefulness of PT formulas for most systems of practical interest, there are some molecular systems where they do break down. These include highly fluxional species “with no structure”, such as  $\text{CH}_5^+$ <sup>10</sup> and  $\text{NO}_3$ .<sup>11</sup> Then, there are cases of intermediate success exemplified by the small and light systems  $\text{H}_3^+$ <sup>12,13</sup> and  $\text{H}_2\text{O}$ ,<sup>14,15</sup> where VPT does not provide an accurate tool for the interpreta-

tion of the measured rovibrational spectra. In these cases, as well as in others where higher accuracy is required from theory, high excitations in the spectra are investigated, the molecule is simply too light, or multiple minima can easily be accessed under the experimental conditions, use of more sophisticated but computationally much more expensive variational quantum mechanical nuclear motion techniques come to the rescue and provide “exact” results within a given potential energy surface (PES).

Experimental investigation of molecular structures of small molecules has also been based on approximate PT approaches and usually on the use of simple normal coordinates or diatomic paradigms, like the Morse oscillator,<sup>16</sup> for the description of the (anharmonic) vibrations. Furthermore, the effect of overall molecular rotation, if treated at all due to its small magnitude at low temperatures, was included in structural studies through simple classical expressions.<sup>17</sup> Following some pioneering studies,<sup>3,18,19</sup> the work of Reitan,<sup>20</sup> Morino,<sup>21,22</sup> Kuchitsu,<sup>23–26</sup> Bartell,<sup>27–32</sup> Herschbach,<sup>33,34</sup> Mills,<sup>26,35</sup> Watson,<sup>36–38</sup> and others<sup>39</sup> started more than 50 years ago resulted in formulas that have been used ever since to determine averaged, sometimes temperature-dependent structural parameters from gas electron diffraction (GED) and rotationally resolved spectroscopy measurements. There have also been attempts, with rather limited success,<sup>28,40–42</sup> to determine equilibrium structures based on the diffraction of high-energy electrons on molecules. Microwave (MW) spectroscopy has been considerably more successful in yielding precise equilibrium structural parameters; the seemingly best technique leads to what is often called nowadays a

<sup>†</sup> Part of the “Walter Thiel Festschrift”.

<sup>‡</sup> Current address: Cherry L. Emerson Center for Scientific Computation and Department of Chemistry, Emory University, Atlanta, Georgia 30322.

semiexperimental equilibrium structure.<sup>43–48</sup> This technique can be used to approximate the equilibrium structures of molecules of the size of amino acids, like glycine<sup>46</sup> and proline,<sup>47</sup> if precise experimental rotational constants are available for a sufficient number of isotopologues. Excellent reviews exist which summarize the perturbational and other approximate approaches of this field,<sup>44,48</sup> which is thus usually considered as mature.

The possibility of the computation of exceedingly accurate adiabatic ab initio PESs for small molecules<sup>49–51</sup> means that determination of *equilibrium* structures to a precision exceeding that of most experiments can be achieved by quantum theory. For a recent example see the investigation of the equilibrium structures of water, reported in the predecessor of this paper.<sup>52</sup> Recent developments in the techniques treating nuclear motion (see, e.g., refs 10 and 53–56) mean, furthermore, that variational studies employing exact kinetic energy operators are not limited any more to small, three- and four-atomic, systems but can be extended to somewhat larger ones including those having large amplitude motion over several minima that can be accessed even at relatively low temperatures. These new developments are expected to result in a renewed interest in the computational structural and spectroscopic studies of “difficult” molecular systems.

The present study, with an eye on similar studies on larger systems, was designed to investigate carefully how the direct quantum mechanical route allows us to move from “static”, purely theoretical equilibrium results to quantities closer in spirit to measurable ones, such as effective and temperature-dependent parameters. Furthermore, as an application, we are providing highly accurate, benchmark-quality data to measurable temperature-dependent effective structures and spectroscopic molecular constants of water. Water was chosen as the model compound of this study for the following reasons: (a) it is perhaps the only polyatomic and polyelectronic molecule for which unusually precise semiglobal ab initio<sup>49,51</sup> (and empirical adiabatic<sup>57</sup>) PESs are available; (b) it is a simple bent triatomic molecule amenable to rigorous treatments for both its electronic and nuclear motions; (c) it is known (see, e.g., ref 14) that perturbation theory in its simplest form does not work well for water; (d) being one of the most important molecules that is also easy to handle experimentally, water has been studied in great detail both by spectroscopy<sup>58–74</sup> and by gas electron diffraction,<sup>75</sup> providing critical anchors when theoretical and experimental results are compared. In a sense, the present study is a continuation of the investigations of Fink and co-workers from the early 1980s on the vibrationally averaged, temperature-dependent structures of CO<sub>2</sub>,<sup>76</sup> SO<sub>2</sub>,<sup>77</sup> and N<sub>2</sub>O,<sup>78</sup> but using state-of-the-art computational technology and a much lighter system for which the perturbational techniques used there are clearly insufficient. Note that variational nuclear motion treatments related to GED have also been performed at about the same time by Hilderbrandt and Kohl<sup>79,80</sup> for SO<sub>2</sub> and CO<sub>2</sub>.

## 2. Computational Details

**2.1. Electronic Structure Calculations.** The adiabatic (mass-dependent) CVRQD PESs<sup>49,51</sup> of the water molecule, generated according to the composite focal-point analysis (FPA) approach<sup>81,82</sup> and employed extensively in this study, are built upon a number of component parts: a complete basis set valence-only (V) surface obtained by extrapolating large basis set internally contracted multireference configuration interaction (ICMRCI) calculations keeping the oxygen 1s orbital frozen, a core–core and core–valence correlation surface to correct for the frozen oxygen 1s orbital in the

ICMRCI calculations (C), relativistic correction surfaces to the electronic kinetic energy and Coulomb interactions (R),<sup>83,84</sup> a quantum electrodynamics (QED) correction surface (Q),<sup>85</sup> and an adiabatic or diagonal Born–Oppenheimer (DBOC) correction surface (D),<sup>49,86</sup>

**2.2. Nuclear Motion and Rovibrational Averaging Calculations.** The six-dimensional variational rovibrational calculations and the rovibrational averagings of this study have been performed with the DOPI3R package.<sup>87,88</sup> DOPI3R is based on one of the simplest possible strategies to compute rovibrational eigenpairs employing a complete, tailor-made triatomic molecular Hamiltonian: the Hamiltonian is expanded in orthogonal (O), e.g., Jacobi<sup>89</sup> or Radau,<sup>90</sup> internal coordinates  $\{R_1, R_2, \Theta\}$ ,<sup>91,92</sup> its matrix,  $\mathbf{H}^{\text{DVR}}$ , is represented by the discrete variable representation (DVR)<sup>93–100</sup> coupled with a product (P) basis, where there is no direct coupling between the radial and angular basis functions, and advantage is taken of the sparsity and special structure of the resulting Hamiltonian matrix whose required eigenvalues and eigenvectors can thus be computed extremely efficiently by variants of iterative (I) techniques, in the present case the Lanczos method.<sup>101</sup> The eigenvectors given in a grid representation can be simply employed for computing expectation values through eq 1; vide infra.

To cover the temperature range 0–1500 K during thermal averaging, rovibrational computations had to be performed up to at least 10 000 cm<sup>-1</sup> above the zero-point energy level. In this study *complete* rovibrational energy levels, wave functions, and the required expectation values were computed up to 15 000 and 11 000 cm<sup>-1</sup> for H<sub>2</sub><sup>16</sup>O and D<sub>2</sub><sup>16</sup>O, respectively, using nuclear masses. The ab initio database generated contains 18 486 (24 415) rovibrational energies, the number of vibrational ( $J = 0$ ) levels is 64 (61), and the computations had to be performed up to  $J = 39$  (45) for H<sub>2</sub><sup>16</sup>O (D<sub>2</sub><sup>16</sup>O), where  $J$  is the rotational quantum number. The efficiency of the DOPI3R package, employing exact kinetic energy operators, is demonstrated by the fact that a large number of converged rovibrational computations could be performed in a matter of days on a standard personal computer.

Computation of the vibrationally averaged rotational constants in the Eckart frame was performed with both the DOPI3R<sup>87,88</sup> and DEWE<sup>53</sup> algorithms and packages, where DEWE stands for DVR representation of the Eckart–Watson Hamiltonian with an exact inclusion of the PES. The results reported herein correspond to those obtained with DOPI3R and employing nuclear masses for the vibrational computations and atomic masses for computing rotational constants. Note that singularities associated with linear configurations hinder the computation of vibrationally averaged rotational constants in both procedures. The wave functions in DOPI3R can be fully converged for all bound states but the formulas for  $A$  and  $B$  are singular at linear structures. In the case of DEWE, even the wave functions corresponding to excited bending states cannot be converged due to the well-known singularity problem of the Eckart–Watson Hamiltonian.

## 3. Theoretical Background

**3.1. Variational Averaging.** Computation of average spectroscopic parameters, including temperature-dependent rovibrationally averaged structural parameters and vibrationally averaged rotational constants, using quantum chemical techniques constitutes several challenges. For perturbative treatments, accurate equilibrium values of these quantities must be available, obtained from electronic structure computations. As to the accurate equilibrium structures and

equilibrium rotational constants of the water molecule, these were recently investigated by us<sup>52</sup> on the basis of the same high-quality CVRQD PESs<sup>49,51</sup> used in this study. Next, one must be able to compute average properties, which can be done via different variational or perturbational routes. For some average quantities an added difficulty is to compare computed and experimental effective parameters as the true meaning of the latter may not be fully evident.

The variational technique to deduce (ro)vibrationally averaged properties is based on simple expectation value computations, where the (ro)vibrational wave functions obtained from variational (or nearly variational) nuclear motion computations are employed to determine expectation values of the given molecular property. The variational technique has several advantages. The function  $f$ , which describes a molecular property, can be given as an arbitrary function of the internal coordinates. Therefore, it is not required to give the form of  $f$  in a Taylor series expansion. The variational vibrational computations provide converged energy levels with the corresponding accurate wave functions. These numerically exact wave functions can be employed for expectation value computations providing exact vibrationally averaged properties. It must also be stressed that the variational technique allows computation of properly rovibrationally averaged properties, artificial separation of the vibrational and rotational degrees of freedom is not necessary.

As noted, determination of the expectation value of an arbitrary function  $f$  requires the computation of the integral  $\langle \Psi_{\nu J_\tau} | f | \Psi_{\nu J_\tau} \rangle$ , where  $\nu$  and  $J_\tau$  stand for the usual vibrational and rotational labels (approximate or good quantum numbers), respectively, and here  $\nu$  is a collective index of normal-mode quantum numbers  $n_1$ ,  $n_2$ , and  $n_3$ , representing the symmetric stretch, bend, and antisymmetric stretch motions of water, respectively,  $J$  is a “good” quantum number corresponding to the overall rotation of the molecule, and  $\tau = K_a - K_c$ , where  $K_a$  and  $K_c$  have their usual meaning, i.e., the values of  $|K|$  for the limiting prolate and oblate symmetric rotor limits, respectively, with which the particular level correlates. Computation of this multidimensional integral becomes especially simple when one works in the discrete variable representation<sup>93–100</sup> of the rovibrational Hamiltonian. For a triatomic molecule, computation of expectation values of a function  $f(R_1, R_2, \cos \Theta)$  in a DVR representation is given simply as

$$\langle f(R_1, R_2, \cos \Theta) \rangle_{\nu J_\tau} = \sum_{n_1, n_2, l=1, K=(0/1)}^{N_1, N_2, L, J} (C_{Kn_1 n_2 l, \nu J_\tau})^2 f(r_{n_1}, r_{n_2}, q_l^K) \quad (1)$$

where the matrix  $\mathbf{C}$  contains the eigenvectors of  $\mathbf{H}^{\text{DVR}}$ , (0/1) refers to (odd/even) parity,  $N_1$ ,  $N_2$ , and  $L$  are the number of the  $R_1$ -,  $R_2$ -, and  $\Theta$ -dependent DVR basis functions, respectively, and  $r_{n_1}$ ,  $r_{n_2}$ , and  $q_l^K$  are the grid points (for further details, see refs 87 and 88). It is important to emphasize that during rovibrational averaging one can take advantage of the fact that the  $f$  function does not depend on the Euler angles that describe the overall rotation of the molecule.

The effect of temperature can be taken into account by simple Boltzmann averaging, for an application see eqs 2 and 3 below.

**3.2. Temperature-Dependent Rovibrationally Averaged Structural Parameters.** At the dawn of modern structural chemistry, especially in the 1960s, it was difficult to compare structural parameters obtained by different gas-phase experimental techniques (see, e.g., the discussions in refs 21–29 and 44). The main difficulty lay in the different vibrational averages

the usual distance definitions characterizing the experimental spectroscopic and diffraction techniques represent. Let us summarize briefly the structure types that have a clear physical meaning and are most relevant for this study.

The equilibrium structure, represented as  $r_e$ , is a purely theoretical construct and accurate Born–Oppenheimer (BO) and adiabatic values,  $r_e^{\text{BO}}$  and  $r_e^{\text{ad}}$ , respectively, can be obtained from a judicious use of modern correlated electronic structure techniques.<sup>52</sup> The  $r_e$  distances correspond to minima on the respective PESs and represent the distances between equilibrium nuclear positions. The  $r_z$  structure, where  $z$  stands for zero-point, is the structure that belongs to the average nuclear positions in the ground vibrational state and, thus, by definition, has no temperature dependence. Next, the two distance types of central importance to this study are discussed,  $r_{g,T}$  and  $r_{a,T}$ , where  $g$  stands for “center of gravity”,  $r_{g,T}$  denotes the thermal average value of an  $r_g$ -type internuclear distance at temperature  $T$ , and the definitions are

$$r_{g,T} = \frac{\sum_{\nu J_\tau} \langle r \rangle_{\nu J_\tau} e^{-(E_{\nu J_\tau} - E_0)/kT}}{\sum_{\nu J_\tau} e^{-(E_{\nu J_\tau} - E_0)/kT}} \quad (2)$$

and

$$r_{a,T} = \frac{\sum_{\nu J_\tau} e^{-(E_{\nu J_\tau} - E_0)/kT}}{\sum_{\nu J_\tau} \langle 1/r \rangle_{\nu J_\tau} e^{-(E_{\nu J_\tau} - E_0)/kT}} \quad (3)$$

In these expressions  $E_0$  is the vibrational zero-point energy,  $E_{\nu J_\tau}$ 's are the (ro)vibrational energies determined in a variational computation,  $k$  is Boltzmann's constant, and the averaging uses the corresponding wave functions determined in the same variational computation. The variational computation of different powers of structural parameters, e.g.,  $\langle r \rangle_{\nu J_\tau}$ , is described as follows. First,  $r$  has to be given as a function of the orthogonal (Jacobi or Radau) coordinates,  $r(R_1, R_2, \cos \Theta)$ . For example, in the case of Jacobi coordinates,  $R_1$  represents a diatomic distance (one of the two OH distances of water) and  $m_O$  and  $m_H$  are the nuclear masses; therefore, in this case  $r(R_1, R_2, \cos \Theta) = R_1$  and  $r(R_1, R_2, \cos \Theta) = \{[m_O/(m_O + m_H)]^2 R_1^2 + R_2^2 - [2m_O/(m_O + m_H)] R_1 R_2 \cos \Theta\}^{1/2}$  for the OH and HH distances, respectively. Second, one can simply use eq 1 for calculating the expectation values:  $\langle r \rangle_{\nu J_\tau} = \langle r(R_1, R_2, \cos \Theta) \rangle_{\nu J_\tau}$ . Gas electron diffraction, for example, results principally in  $r_{a,T}$  and  $r_{g,T}$  structures that can deviate substantially from the equilibrium  $r_e$  structures and from each other. In this work, expectation value symbols will be retained to denote variationally computed expectation values of structural parameters. Thus, vibrationally averaged distances  $\langle r \rangle_\nu$  correspond to the  $\nu$ th vibrational state and rovibrationally averaged distances  $\langle r \rangle_{\nu J_\tau}$  correspond to the rovibrational state characterized by the labels  $\nu$  and  $J_\tau$ .

Next, a few words about rotational contributions to effective distances. The traditional way to incorporate rotational motion in the distance definition goes through a classical mechanical approximation,<sup>17,22</sup> which gives a linear temperature dependence in the rotational contribution to the averaged distance,

$$\langle \delta r \rangle_{\text{rot}}^T = \sigma T \quad (4)$$



The variational technique provides an alternative, fully quantum mechanical way to deal with the rotational contribution through exact rovibrational computations, as given in eqs 2 and 3.

Finally, a few words about other distance types not directly relevant for this study. The  $r_0$  distances are determined from effective ground-state rotational constants (like  $B_0^\xi$ , where  $\xi = a, b, c$  are the inertial axes) obtained from spectroscopic [usually microwave and millimeterwave] measurements. The contributions of the zero-point vibrations to  $B_0^\xi$  often cause inconsistencies and anomalies in the  $r_0$  distances determined. Therefore, various strategies have been advanced to cure such problems. For example, an  $r_s$ , so-called substitution, structure determination has been developed by spectroscopists.<sup>102–104</sup> It has no clear physical meaning and thus it is considered no further in this study. The mass-dependence molecular structures,  $r_m^{(1)}$  and  $r_m^{(2)}$  of Watson,<sup>38</sup> provide another set of estimates to the true equilibrium structures of molecules but these again are not considered here further. It is only mentioned that empirical  $r_s$ -type,<sup>105</sup>  $r_m^{(2)}$ -type,<sup>38</sup> and  $r_z$ -type<sup>26</sup> estimates of the equilibrium structure of the water molecule have been reported.

**3.3. Vibrationally Averaged Rotational Constants.** Effective rotational constants, incorporating vibrational averaging, are the principal structural results obtained from fitting appropriate rovibrational Hamiltonians to usually MW and MMW but also infrared (IR) spectroscopic data. The average rotational constants  $A_\nu$ ,  $B_\nu$ , and  $C_\nu$ , determined experimentally, correspond to the  $\nu$ th vibrational state. “Experimental” rotational constants of water can differ appreciably, on the order of  $0.1 \text{ cm}^{-1}$  with maximum deviations around  $0.3 \text{ cm}^{-1}$ , from each other, depending principally on the type of Hamiltonian used for their determination and the input set of energy levels. One can determine vibrationally averaged rotational constants based on theoretical computations basically in two ways.

The traditional route goes through VPT2 formulas.<sup>2–8</sup> The effective rotational constants, for example the constant  $B$  of a nonlinear triatomic molecule, in the  $\nu$ -th vibrational state, having  $(n_1 n_2 n_3)$  quanta in the three vibrational modes, depend on the equilibrium constants and are given by expressions of the form

$$B_\nu = B_e - \sum_{i=1}^3 \alpha_i^B (n_i + d_i/2) + \sum_{i \geq j}^3 \gamma_{ij}^B (n_i + d_i/2)(n_j + d_j/2) + \dots \quad (5)$$

where  $d_i$  denote degeneracies and  $\alpha$ , the so-called vibration–rotation interaction constants, can be obtained through simple formulas from a cubic normal-coordinate force field expansion of the potential,<sup>6,7</sup> while  $\gamma$  is the next higher-order analogue for which similar formulas have also been derived.<sup>106</sup> There are only very few cases where the  $\gamma$  constants have been determined experimentally; these include mostly linear molecules. It is generally accepted that the  $\alpha$  constants are reliable if the  $\gamma$  constants are about 2 orders of magnitude smaller (in these cases the  $\alpha$ 's are also about 2 orders of magnitude smaller than the rotational constants).

The second route, more to the heart of the present work, computes effective spectroscopic constants, including rotational constants, as expectation values employing (ro)vibrational wave functions from variational nuclear motion calculations. This route is discussed in some detail below.

An effective rotational Hamiltonian used in the evaluation of high-resolution rotation-vibration experiments<sup>107</sup> may have the form of, for instance,

$$\hat{H}_{\text{eff},\nu}^{\text{rot}} = A_\nu \hat{J}_x^2 + B_\nu \hat{J}_y^2 + C_\nu \hat{J}_z^2 + \sum_{\beta\gamma} T_\nu^{\beta\gamma} (\hat{J}_\beta^2 + \hat{J}_\gamma^2)^2 + \dots \quad (6)$$

where  $A_\nu$ ,  $B_\nu$ ,  $C_\nu$ , and  $T_\nu^{\beta\gamma}$  ( $\beta, \gamma = x, y, z$ ) are so-called spectroscopic constants corresponding to a given vibrational state  $\nu$ . To predict effective spectroscopic constants from variational nuclear motion computations, one should mimic the procedure used by spectroscopists leading to effective rotational Hamiltonians. Such a procedure was suggested, for example, by Lukka and Kauppi.<sup>108</sup> Within their proposed algorithm one has to (a) start from an arbitrary (hopefully exact) rotation–vibration Hamiltonian, (b) compute vibration-only wave functions, (c) carry out vibrational averaging of the total rotation–vibration Hamiltonian using the computed wave functions, and (d) use a series of numerical contact transformations to convert the effective Hamiltonian to the expected form given in eq 6. While this procedure is certainly a very useful though hardly explored one to bridge high-quality theory and experiment, it is not followed here.

A more straightforward and simpler theoretical route is followed in which the Eckart frame<sup>18</sup> is used in the variational computations. It should be stressed at the outset that this route does not lead to constants that can be compared directly with experimental effective spectroscopic constants but provides a theoretically sound starting point for such comparisons. The choice of the Eckart frame means that the rotation–vibration interaction is zero at the reference structure and it is very small close to the reference structure. (Note that it is impossible to define a frame in which the rotation–vibration interaction vanishes over a finite region of the configuration space.<sup>109</sup>) The use of the Eckart frame is one of the best choices if maximal rotation–vibrational separation is to be achieved, the coupling terms are small for lower vibrational excitations of not too wide-amplitude motions. Using the Eckart frame and universally defined rectilinear internal coordinates (normal coordinates), the rotation–vibration Hamiltonian can be simplified to the Eckart–Watson form<sup>110</sup>

$$\hat{H}^{\text{vib-rot}} = \frac{1}{2} \sum_{\alpha\beta} (\hat{J}_\alpha - \hat{\pi}_\alpha) \mu_{\alpha\beta} (\hat{J}_\beta - \hat{\pi}_\beta) + \frac{1}{2} \sum_{k=1}^{3N-6} \hat{p}_k^2 - \frac{\hbar^2}{8} \sum_{\alpha} \mu_{\alpha\alpha} + V \quad (7)$$

with volume element  $dQ_1 dQ_2 \dots dQ_{3N-6} \sin\theta d\varphi d\theta d\chi$ , where  $\varphi$ ,  $\theta$ , and  $\chi$  are the Euler angles. Rectilinear internal (normal) coordinates are specified as

$$Q_k = \sum_{i=1}^N \sum_{\alpha\beta\gamma} \sqrt{m_i} l_{i\alpha k} (x_{i\alpha} - c_{i\alpha}) \quad k = 1, 2, \dots, 3N - 6 \quad (8)$$

where  $m_i$  is the mass associated with the  $i$ th nuclei,  $c_{i\alpha}$  corresponds to the nonlinear reference structure, and  $x_{i\alpha}$  are the instantaneous Cartesian coordinates in the Eckart frame. The usage of the Eckart frame and the orthogonality requirement of Watson imposes the following conditions on the elements  $l_{i\alpha k}$  specifying the actual rectilinear internal coordinates

$$\sum_{i=1}^N \mathbf{I}_{ik}^T \mathbf{l}_{il} = \delta_{kl} \quad \sum_{i=1}^N \sqrt{m_i} \mathbf{l}_{ik} = \mathbf{0} \quad \sum_{i=1}^N \sqrt{m_i} \mathbf{c}_i \times \mathbf{l}_{ik} = \mathbf{0} \quad (9)$$

In eq 7,  $\hat{P}_k = i\hbar\partial/\partial Q_k$  ( $k = 1, 2, \dots, 3N - 6$ ),  $\hat{J}_x$ ,  $\hat{J}_y$ , and  $\hat{J}_z$  are the components of the total angular momentum,  $\hat{\pi}_\alpha = \sum_{kl=1}^{3N-6} \zeta_{kl}^\alpha Q_k \hat{P}_l$  is the Coriolis coupling operator,  $\mu_{\alpha\beta} = (\mathbf{I}^{-1})_{\alpha\beta}$  is the generalized inverse inertia tensor,  $I_{\alpha\beta} = \sum_{klm=1}^{3N-6} \zeta_{km}^\alpha \zeta_{lm}^\beta Q_k Q_l$  is the generalized inertia tensor, and  $\zeta_{km}^\alpha = e_{\alpha\beta\gamma} \sum_{i=1}^N l_{i\beta k} l_{i\gamma m}$ , where  $e_{\alpha\beta\gamma}$  denotes the Lévi-Civita symbol. The vibration-only part of the Eckart–Watson operator has the form

$$\hat{H}^{\text{vib}} = \frac{1}{2} \sum_{\alpha\beta} \hat{\pi}_\alpha \mu_{\alpha\beta} \hat{\pi}_\beta + \frac{1}{2} \sum_{k=1}^{3N-6} \hat{P}_k^2 - \frac{\hbar^2}{8} \sum_{\alpha} \mu_{\alpha\alpha} + V \quad (10)$$

Let us denote the eigenvalues and eigenvectors of  $\hat{H}^{\text{vib}}$  by  $E_v^{\text{vib}}$  and  $\psi_v^{\text{vib}}$ , respectively. By use of the vibrational eigenfunctions, effective rotational operators can be produced by averaging  $\hat{H}^{\text{vib-rot}}$  for each vibrational state as

$$\begin{aligned} \langle \hat{H}^{\text{vib-rot}} \rangle_v &= E_v^{\text{vib}} - \frac{1}{2} \sum_{\alpha\beta} \hat{J}_\alpha \langle \mu_{\alpha\beta} \hat{\pi}_\beta \rangle_v - \\ &\quad \frac{1}{2} \sum_{\alpha\beta} \langle \hat{\pi}_\alpha \mu_{\alpha\beta} \rangle_v \hat{J}_\beta + \frac{1}{2} \sum_{\alpha\beta} \hat{J}_\alpha \langle \mu_{\alpha\beta} \rangle_v \hat{J}_\beta \\ &= E_v^{\text{vib}} - \sum_{\alpha\beta} \langle \hat{\pi}_\alpha \mu_{\alpha\beta} \rangle_v \hat{J}_\beta + \frac{1}{2} \sum_{\alpha\beta} \hat{J}_\alpha \langle \mu_{\alpha\beta} \rangle_v \hat{J}_\beta \end{aligned} \quad (11)$$

where the notation  $\langle \hat{O} \rangle_v = \langle \psi_v^{\text{vib}} | \hat{O} | \psi_v^{\text{vib}} \rangle$  was used for convenience.

For any triatomic molecule, if the Eckart reference structure is expressed in the principal axis frame and the reference lies in the  $x$ – $y$  plane,  $\hat{\pi}_x = \hat{\pi}_y = 0$  and  $\mu_{xz} = \mu_{zx} = \mu_{yz} = \mu_{zy} = 0$ , thus the  $v$ th effective rotational operator simplifies to

$$\langle \hat{H}^{\text{vib-rot}} \rangle_v = E_v^{\text{vib}} - \langle \hat{\pi}_z \mu_{zz} \rangle_v \hat{J}_z + \frac{1}{2} \sum_{\alpha} \langle \mu_{\alpha\alpha} \rangle_v \hat{J}_\alpha^2 + \frac{1}{2} \langle \mu_{xy} \rangle_v (\hat{J}_x \hat{J}_y + \hat{J}_y \hat{J}_x) \quad (12)$$

In what follows the second and fourth terms, corresponding to the Coriolis coupling and the off-diagonal rotational terms, respectively, are not considered, thus

$$\langle \hat{H}^{\text{vib-rot}} \rangle_v \approx E_v^{\text{vib}} + \frac{\langle \mu_{xx} \rangle_v}{2} \hat{J}_x^2 + \frac{\langle \mu_{yy} \rangle_v}{2} \hat{J}_y^2 + \frac{\langle \mu_{zz} \rangle_v}{2} \hat{J}_z^2 \quad (13)$$

Using this form, the spectroscopic constants, called rotational constants, are estimated as

$$A_v \approx \frac{\langle \mu_{xx} \rangle_v}{2} \quad B_v \approx \frac{\langle \mu_{yy} \rangle_v}{2} \quad C_v \approx \frac{\langle \mu_{zz} \rangle_v}{2} \quad (14)$$

Due to their construction, for lower vibrational states these estimates are expected to perform quite well. Nevertheless, neglect of the Coriolis coupling will affect the computed  $C$

constants, corresponding to the out-of-plane axis, making them incompatible with the experimental effective rotational constants.

Next, computation of the vibrationally averaged diagonal elements of the generalized inverse inertia tensor must be considered. If the DEWE protocol and program<sup>53</sup> is used, the generalized inverse inertia tensor,  $\mu_{\alpha\beta}(Q_1, Q_2, \dots, Q_{3N-6})$  ( $\alpha, \beta = x, y, z$ ) is evaluated at every quadrature point; thus if the vibrational wave functions are also evaluated, the computation of the required  $A_v$ ,  $B_v$ , and  $C_v$  estimates from eq 14 is straightforward. To compute the elements of the generalized inverse inertia tensor using arbitrary internal coordinates for triatomic or larger molecules, the following steps must be followed. First, the masses associated with the nuclei and the reference structure fixing the Eckart frame must be defined. It is best to orient the reference structure as dictated by the principal axes of the system. Second, the Cartesian coordinates are to be evaluated in terms of the instantaneous internal coordinates in an arbitrary frame, e.g., by using a  $\mathbf{Z}$ -matrix reader. Third, the instantaneous Cartesian coordinates are transformed, by constructing an appropriate rotational matrix, to Eckart coordinates, which fulfill the Eckart conditions. Fourth, an  $\mathbf{I}$  matrix must be constructed meeting the requirements given in eq 9, and rectilinear internal coordinates,  $Q_k$  ( $k = 1, 2, \dots, 3N - 6$ ), must be evaluated by using eq 8. Fifth, elements of  $\mu_{\alpha\beta}$  are computed according to formulas given below eqs 9.

Thus, DEWE-type algorithms can compute effective rotational constants for semirigid molecules of arbitrary size using the procedure just described. For triatomic molecules or atom-linear molecule complexes, Ernesti and Hutson<sup>111</sup> presented explicit formulas for the same expectation value computations. Their formulas are expressed in terms of Jacobi coordinates, often used by tailor-made triatomic variational nuclear motion codes such as DOPI3R,<sup>87,88</sup> and take proper account of the Eckart conditions. These formulas, in their full form including what Ernesti and Hutson called Coriolis contribution, have been programmed into DOPI3R and they resulted in exactly the same effective rotational constants as obtained with DEWE. The arguments given above explain why the  $C$  rotational constants computed by Ernesti and Hutson for Ar–CO<sub>2</sub> deviate from their eigenvalue fitting counterparts while the  $A$  and  $B$  constants show excellent agreement.

#### 4. Results and Discussion

The computational structural results of this study are summarized in Tables 1–3. Table 1 contains various vibrationally averaged distance and angle parameters. Following Herschbach and Laurie,<sup>33</sup> the distance types, contained in Table 1, related to  $\langle r \rangle$ ,  $\langle r^{-1} \rangle$ ,  $\langle r^2 \rangle$ ,  $\langle r^{-2} \rangle$ ,  $\langle r^3 \rangle$ , and  $\langle r^{-3} \rangle$  will be denoted as “mean”, “inverse”, “rms”, “effective”, “cubic”, and “inverse cubic”, respectively. Of course, these definitions can be extended to angles, as well. In general, the averages may represent thermal averages over a Boltzmann (ro)vibrational distribution or averages in any (ro)vibrational state. The temperature dependence of the  $r_g$  (mean internuclear) and  $r_a$  (inverse internuclear) distances is given in Table 2, up to 1500 K, based on variationally computed wave functions and Boltzmann averaging as given in eqs 2 and 3. Table 3 contains parameters related to GED structural studies, namely root-mean-square (rms) amplitudes ( $l_g$ ) and  $\kappa$  anharmonicity parameters, again up to 1500 K. Some of the structural results of this study are also presented graphically; see Figures 1–4. First-principles vibrationally averaged rotational constants of this study, obtained in the Eckart system, are given in Tables 4 and 5 for H<sub>2</sub><sup>16</sup>O and D<sub>2</sub><sup>16</sup>O, respectively. Table 6 contains vibration–rotation interaction

**TABLE 1: Vibrationally Averaged Bond Lengths ( $r$  in Å) and Bond Angles ( $\alpha$  in degrees) of the  $\text{H}_2^{16}\text{O}$  and  $\text{D}_2^{16}\text{O}$  Isotopologues of Water in Different Vibrational States ( $v$ )<sup>a</sup>**

$v$	$\text{H}_2^{16}\text{O}^b$						$\text{D}_2^{16}\text{O}^c$							
	$\langle r_{\text{OH}} \rangle$	$\langle r_{\text{OH}}^2 \rangle^{1/2}$	$\langle r_{\text{OH}}^3 \rangle^{1/3}$	$\langle r_{\text{OH}}^{-1} \rangle^{-1}$	$\langle r_{\text{OH}}^{-2} \rangle^{-1/2}$	$\langle r_{\text{OH}}^{-3} \rangle^{-1/3}$	$\langle \alpha_{\text{HOH}} \rangle$	$\langle r_{\text{OD}} \rangle$	$\langle r_{\text{OD}}^2 \rangle^{1/2}$	$\langle r_{\text{OD}}^3 \rangle^{1/3}$	$\langle r_{\text{OD}}^{-1} \rangle^{-1}$	$\langle r_{\text{OD}}^{-2} \rangle^{-1/2}$	$\langle r_{\text{OD}}^{-3} \rangle^{-1/3}$	$\langle \alpha_{\text{ODD}} \rangle$
(0 0 0)	0.97565	0.97809	0.98052	0.97079	0.96835	0.96592	104.430	0.97077	0.97253	0.97430	0.96724	0.96547	0.96371	104.408
(0 1 0)	0.97805	0.98052	0.98300	0.97311	0.97063	0.96816	105.641	0.97253	0.97431	0.97610	0.96896	0.96718	0.96539	105.235
(0 2 0)	0.98029	0.98281	0.98534	0.97523	0.97271	0.97019	107.059	0.97423	0.97605	0.97786	0.97060	0.96878	0.96697	106.159
(1 0 0)	0.99252	0.99745	1.00235	0.98264	0.97773	0.97287	104.130	0.98276	0.98630	0.98984	0.97565	0.97212	0.96861	104.291
(0 0 1)	0.99301	0.99797	1.00291	0.98307	0.97814	0.97325	103.372	0.98339	0.98698	0.99055	0.97621	0.97263	0.96908	103.527
(0 3 0)	0.98227	0.98486	0.98745	0.97709	0.97451	0.97192	108.763	0.97584	0.97770	0.97956	0.97213	0.97027	0.96842	107.206
(1 1 0)	0.99502	0.99999	1.00493	0.98507	0.98013	0.97524	105.267	0.98453	0.98809	0.99164	0.97742	0.97388	0.97036	105.081
(0 1 1)	0.99562	1.00064	1.00563	0.98558	0.98059	0.97566	104.465	0.98526	0.98888	0.99248	0.97803	0.97443	0.97086	104.292
(0 4 0)	0.98386	0.98652	0.98917	0.97855	0.97590	0.97325	110.899	0.97732	0.97922	0.98112	0.97351	0.97161	0.96971	108.409

<sup>a</sup> Based on variational nuclear motion computations using an exact kinetic energy operator, the CVRQD PESs of refs 49 and 51, and the DOPI3R program system. <sup>b</sup> The corresponding equilibrium structural parameters are  $r_{\text{eq}}^{\text{ad}}(\text{OH}) = 0.95785$  Å and  $\alpha_{\text{c}}(\text{HOH}) = 104.50^\circ$ . <sup>c</sup> The corresponding equilibrium structural parameters are  $r_{\text{eq}}^{\text{ad}}(\text{OD}) = 0.95783$  Å and  $\alpha_{\text{c}}(\text{DOD}) = 104.49^\circ$ .

constants of different order for the  $\text{H}_2^{16}\text{O}$  isotopologue. The normal-mode labels used in Tables 1, 4, and 5 correspond to those given in refs 112 and 113.

**4.1. Structural Parameters.** As clear from Table 1, vibrational averaging based on variationally computed wave functions can be performed using arbitrary functions of the internuclear coordinates  $r$  and these yield significantly different results for different powers of  $r$ . The average OX distances ( $X = \text{H}$  or  $\text{D}$ ) based on different moments deviate substantially from each other. As suggested by simple perturbative estimates, the order of the distances is  $\langle r^3 \rangle^{1/3} > \langle r^2 \rangle^{1/2} > \langle r \rangle > \langle r^{-1} \rangle^{-1} > \langle r^{-2} \rangle^{-1/2} > \langle r^{-3} \rangle^{-1/3} > r_{\text{e}}$ . It is noteworthy that while the equilibrium OH and OD bond lengths in the adiabatic approximation are almost the same, differing from each other only by  $0.000\,02$  Å,<sup>52</sup>  $\langle r(\text{OH}) \rangle_0$  is longer than  $\langle r(\text{OD}) \rangle_0$  by a substantial  $0.004\,88$  Å, where  $\langle r \rangle_0$  denotes the vibrational ground state. At the same time, the  $0.01^\circ$  difference in the equilibrium HOH and DOD bond angles changes very little: it increases only to  $0.02^\circ$  in the ground vibrational state. It is thus remarkable how fast the average bond angle increases with the  $n_2$  bending quantum number. For the (0 4 0) vibrational state the HOH and DOD bond angles open up by  $6.5^\circ$  and  $4.0^\circ$ , respectively, resulting in an angle larger than the tetrahedral angle in the former case. The regularities in  $\langle \Delta\alpha(\text{HOH}) \rangle$  and  $\langle \Delta\alpha(\text{DOD}) \rangle$  on the bending and stretching excitations can clearly be seen on the two panels of Figure 1. Remarkably, if the bending mode is excited above the barrier to linearity,<sup>114,115</sup> the average bond angle starts decreasing. The isotopic effect on the effective bond angle is also quite remarkable, in many cases considerably more pronounced than that for the bond length.

Traditionally, chemists interested in the structures of molecules in the gas phase often employed perturbation theory (PT) and arguments based on the Morse oscillator approximation to understand and model anharmonic vibrations of molecules. The principal advantage of the Morse potential,  $V(x) = D[1 - \exp(-ax)]^2$ , where  $D$  is the dissociation energy, for GED studies was that it allowed the treatment of the anharmonic vibrations of all internuclear distances in terms of a single Morse parameter,  $a$ . Simple perturbative arguments suggest that  $\langle x \rangle = \frac{3}{2}a\langle x^2 \rangle$  or more precisely, going to higher order,  $\langle x \rangle = \frac{3}{2}a\langle x^2 \rangle - \frac{7}{16}a^2\langle x^3 \rangle$ , where  $x = r - r_{\text{e}}$ . The present results show the approximate validity of these simple and often used approximations over the different vibrational states. Nevertheless, the bonded  $a/\text{Å}^{-1}$  values that can be deduced for the different vibrational states of  $\text{H}_2^{16}\text{O}(\text{D}_2^{16}\text{O})$  cover the region from 2.10 (2.19) [for the (1 0 0) state] to 2.93 (3.17) [for the (0 4 0) state]. Furthermore, as Bartell showed,<sup>27</sup> the approximate relation based on PT between  $r_{\text{a}}$  and  $r_{\text{g}}$  is  $r_{\text{a}} = r_{\text{g}} - l_{\text{g}}^2/r$ , where  $l_{\text{g}} = (\langle r^2 \rangle - \langle r \rangle^2)^{1/2}$  is the root-mean-square (rms) amplitude. As the data in Table 1 demonstrate, this relationship holds very well. It is interesting to note also that the  $r_{\text{g},0} - r_{\text{a},0}$  difference is accidentally basically the same as the  $r_{\text{g},0}(\text{OH}) - r_{\text{g},0}(\text{OD})$  isotopic effect.

Next, let us discuss the computed data related to GED experiments, performed for water by Shibata and Bartell<sup>75</sup> more than 40 years ago. The experiments were executed at  $29^\circ\text{C}$ , which is approximated as  $300\text{ K}$  here. The temperature-dependent quantities  $r_{\text{a}}$  ( $r_{\text{g}}$ ),  $l_{\text{g}}^2$ , and  $\kappa$  are the three kinds of adjustable parameters that can be refined during conventional GED structure analyses. Note that Shibata and Bartell did not include  $\kappa$ 's in their structural refinements. The  $r_{\text{a}}$  ( $r_{\text{g}}$ ) parameters of the present study have already been discussed at some length, the  $300\text{ K}$  values can be found in Table 2. In Table 2 of ref 75, GED parameters obtained from the radial distribution curve and

**TABLE 2: Temperature Dependence of the Average Internuclear ( $r_g$ ) and Inverse Internuclear ( $r_a$ ) Structural Parameters (in Å) of the  $\text{H}_2^{16}\text{O}$  and  $\text{D}_2^{16}\text{O}$  Molecules<sup>a,b</sup>**

T/K	$r_g(\text{OH})$		$r_g(\text{HH})$		$r_g(\text{OD})$		$r_g(\text{DD})$	
	$J = 0$	$J \geq 0$	$J = 0$	$J \geq 0$	$J = 0$	$J \geq 0$	$J = 0$	$J \geq 0$
0	0.97565	0.97565	1.53823	1.53823	0.97077	0.97077	1.53128	1.53128
100	0.97565	0.97584	1.53823	1.53819	0.97077	0.97096	1.53128	1.53125
200	0.97565	0.97605	1.53823	1.53815	0.97077	0.97116	1.53128	1.53122
300	0.97566	0.97625	1.53824	1.53812	0.97077	0.97136	1.53129	1.53122
400	0.97566	0.97646	1.53825	1.53810	0.97079	0.97158	1.53133	1.53125
500	0.97568	0.97669	1.53830	1.53812	0.97084	0.97183	1.53142	1.53132
600	0.97571	0.97692	1.53837	1.53817	0.97091	0.97211	1.53157	1.53145
700	0.97577	0.97718	1.53849	1.53825	0.97103	0.97242	1.53178	1.53163
800	0.97584	0.97747	1.53865	1.53838	0.97119	0.97279	1.53205	1.53188
900	0.97595	0.97778	1.53886	1.53856	0.97141	0.97321	1.53240	1.53220
1000	0.97609	0.97813	1.53913	1.53879	0.97167	0.97368	1.53282	1.53259
1100	0.97627	0.97852	1.53945	1.53907	0.97197	0.97420	1.53330	1.53303
1200	0.97648	0.97895	1.53982	1.53940	0.97232	0.97476	1.53384	1.53353
1300	0.97674	0.97942	1.54026	1.53978	0.97271	0.97536	1.53444	1.53408
1400	0.97702	0.97993	1.54075	1.54022	0.97313	0.97600	1.53508	1.53467
1500	0.97735	0.98048	1.54129	1.54070	0.97358	0.97666	1.53578	1.53529

T/K	$r_a(\text{OH})$		$r_a(\text{HH})$		$r_a(\text{OD})$		$r_a(\text{DD})$	
	$J = 0$	$J \geq 0$	$J = 0$	$J \geq 0$	$J = 0$	$J \geq 0$	$J = 0$	$J \geq 0$
0	0.97079	0.97079	1.52968	1.52968	0.96724	0.96724	1.52524	1.52524
100	0.97079	0.97098	1.52968	1.52963	0.96724	0.96743	1.52524	1.52521
200	0.97079	0.97118	1.52968	1.52960	0.96724	0.96763	1.52524	1.52519
300	0.97079	0.97138	1.52967	1.52956	0.96724	0.96783	1.52523	1.52516
400	0.97080	0.97159	1.52967	1.52953	0.96726	0.96805	1.52519	1.52511
500	0.97081	0.97181	1.52964	1.52948	0.96730	0.96829	1.52514	1.52505
600	0.97084	0.97204	1.52961	1.52941	0.96737	0.96856	1.52508	1.52497
700	0.97089	0.97230	1.52956	1.52934	0.96747	0.96885	1.52503	1.52491
800	0.97096	0.97257	1.52952	1.52928	0.96760	0.96919	1.52501	1.52487
900	0.97105	0.97286	1.52949	1.52922	0.96777	0.96956	1.52502	1.52486
1000	0.97117	0.97319	1.52947	1.52917	0.96798	0.96997	1.52507	1.52488
1100	0.97131	0.97354	1.52949	1.52915	0.96821	0.97042	1.52516	1.52494
1200	0.97148	0.97392	1.52953	1.52916	0.96848	0.97090	1.52528	1.52503
1300	0.97167	0.97433	1.52960	1.52919	0.96878	0.97140	1.52544	1.52516
1400	0.97190	0.97477	1.52970	1.52925	0.96910	0.97193	1.52563	1.52531
1500	0.97214	0.97523	1.52984	1.52935	0.96945	0.97247	1.52586	1.52548

<sup>a</sup> See footnote *a* to Table 1. The equilibrium structural parameters are  $r_{\text{eq}}^{\text{ad}}(\text{OH}) = 0.95785 \text{ \AA}$ ,  $r_{\text{eq}}^{\text{ad}}(\text{HH}) = 1.51472 \text{ \AA}$ ,  $r_{\text{eq}}^{\text{ad}}(\text{OD}) = 0.95783 \text{ \AA}$ , and  $r_{\text{eq}}^{\text{ad}}(\text{DD}) = 1.51460 \text{ \AA}$ .  $T$  is the temperature.  $J$  is the rotational quantum number and thus “ $J = 0$ ” refers to pure vibrational averaging while “ $J \geq 0$ ” corresponds to proper rovibrational averaging. <sup>b</sup> All the digits reported are significant under 1000 K, above it the results may have an uncertainty of about  $(1-2) \times 10^{-5} \text{ \AA}$ .

from a “smooth atomic background” are given. These deviate substantially from each other, background variations resulted in changes as large as  $0.004 \text{ \AA}$  for  $\text{H}_2^{16}\text{O}$ . The final results of Shibata and Bartell,<sup>75</sup> called “derived parameters”, are given in their Table 3, and these will be used for comparison in what follows. These GED-derived structural parameters for the bonded atoms agree very well with the much more precise, and presumably accurate, ab initio estimates of this study. The GED (ab initio)  $r_a(\text{OH})$  and  $r_g(\text{OH})$  results are  $0.9716$  ( $0.9714$ ) and  $0.9763$  ( $0.9763$ ) Å, respectively. Given that the GED uncertainties were said to be<sup>75</sup> of the order of  $0.003 \text{ \AA}$ , the agreement seems fortuitously good. The same numbers for  $r_a(\text{OD})$  and  $r_g(\text{OD})$  are  $0.9664$  ( $0.9678$ ) and  $0.9700$  ( $0.9714$ ) Å, respectively, which still represent excellent agreement. As expected, due to the small scattering power of H (and D), the agreement for the HH and DD structural parameters is much worse. The GED (ab initio)  $r_a(\text{HH})$  and  $r_g(\text{HH})$  results are  $1.559$  ( $1.5296$ ) and  $1.567$  ( $1.5381$ ) Å. With the moments obtained in this study and presented in Table 1, the mean-square amplitudes can be given as  $l_g^2 = \langle (x - \langle x \rangle)^2 \rangle = \langle x^2 \rangle - \langle x \rangle^2 = \langle r^2 \rangle - \langle r \rangle^2$ . One obtains the following mean-square amplitudes at 300 K,  $l_{g,300}(\text{OH}) = 0.0690 \text{ \AA}$  and  $l_{g,300}(\text{OD}) = 0.0586 \text{ \AA}$ . These values can be compared with their experimental, 302 K counterparts determined by

Shibata and Bartell,  $0.067(3)$  and  $0.056(2) \text{ \AA}$ , respectively, and thus they show good agreement. This is especially so if one notes the uncertainty of the experimental  $l_g$  values and that it has been estimated that the finite sample size may result in corrections to the experimental rms amplitudes on the order of  $0.01 \text{ \AA}$ .<sup>116</sup>

As the data presented in Tables 2 and 3 show, the variational computations performed in this study allow high-quality predictions for all the important parameters which could be determined in a set of temperature-dependent GED experiments. In Table 2,  $r_g$ - and  $r_a$ -type distances are given for the OX and XX (X = H or D) distances. The distances in the  $J \geq 0$  column should be compared to the experimental values if they were ever determined. As clear from this table and from the associated Figure 2, the change in the OH(OD) bond lengths between room temperature (300 K) and even 1500 K is significant but not large, about  $0.004$  ( $0.005$ ) Å. In GED it is usual to define the so-called anharmonicity parameter as  $\kappa \cong 1/6(\langle x^3 \rangle - 3\langle x \rangle \langle x^2 \rangle)$  (or in the simplest case  $\kappa \cong 1/6\langle x^3 \rangle$ ).<sup>23</sup> The temperature dependence of the  $l_g$  and  $\kappa$  parameters, as well as the rotational contributions to these parameters, can be followed in both Table 3 and Figure 3. Unfortunately, even given the higher quality of modern GED experiments as compared to what was feasible



**TABLE 3: Temperature Dependence of the Root-Mean-Square Amplitude,  $l_g/\text{Å}$ , and the Anharmonicity,  $\kappa/(10^{-6} \text{ Å}^3)$ , Parameters of the  $\text{H}_2^{16}\text{O}$  and  $\text{D}_2^{16}\text{O}$  Molecules<sup>a</sup>**

<i>T/K</i>	$l_g(\text{OH})$		$l_g(\text{HH})$		$l_g(\text{OD})$		$l_g(\text{DD})$	
	$J = 0$	$J \geq 0$	$J = 0$	$J \geq 0$	$J = 0$	$J \geq 0$	$J = 0$	$J \geq 0$
0	0.0690	0.0690	0.1142	0.1142	0.0586	0.0586	0.0958	0.0958
100	0.0690	0.0690	0.1142	0.1141	0.0586	0.0586	0.0958	0.0958
200	0.0690	0.0690	0.1142	0.1141	0.0586	0.0586	0.0958	0.0958
300	0.0690	0.0690	0.1142	0.1141	0.0586	0.0586	0.0960	0.0959
400	0.0690	0.0690	0.1143	0.1142	0.0586	0.0586	0.0965	0.0964
500	0.0690	0.0690	0.1147	0.1145	0.0586	0.0587	0.0974	0.0972
600	0.0690	0.0691	0.1153	0.1151	0.0587	0.0587	0.0986	0.0985
700	0.0690	0.0691	0.1161	0.1159	0.0588	0.0589	0.1002	0.1000
800	0.0691	0.0692	0.1172	0.1169	0.0590	0.0591	0.1020	0.1017
900	0.0692	0.0693	0.1184	0.1181	0.0593	0.0594	0.1040	0.1037
1000	0.0693	0.0695	0.1199	0.1195	0.0597	0.0598	0.1061	0.1057
1100	0.0695	0.0697	0.1214	0.1210	0.0602	0.0603	0.1084	0.1079
1200	0.0698	0.0700	0.1231	0.1226	0.0607	0.0609	0.1107	0.1102
1300	0.0701	0.0704	0.1249	0.1243	0.0613	0.0616	0.1131	0.1125
1400	0.0705	0.0708	0.1268	0.1261	0.0620	0.0623	0.1156	0.1148
1500	0.0709	0.0713	0.1288	0.1280	0.0627	0.0630	0.1180	0.1172

<i>T/K</i>	$\kappa(\text{OH})$		$\kappa(\text{HH})$		$\kappa(\text{OD})$		$\kappa(\text{DD})$	
	$J = 0$	$J \geq 0$	$J = 0$	$J \geq 0$	$J = 0$	$J \geq 0$	$J = 0$	$J \geq 0$
0	7.0	7.0	-1.7	-1.7	3.8	3.8	-0.2	-0.2
100	7.0	6.8	-1.7	-1.3	3.8	3.8	-0.2	-0.2
200	7.0	6.7	-1.7	-1.3	3.8	3.8	-0.2	-0.2
300	7.0	6.6	-1.8	-1.4	3.8	3.7	-0.3	-0.3
400	7.0	6.6	-1.9	-1.5	3.8	3.7	-0.6	-0.6
500	7.0	6.5	-2.3	-1.9	3.8	3.6	-1.2	-1.2
600	7.0	6.4	-2.9	-2.6	3.8	3.6	-2.0	-2.1
700	7.0	6.3	-3.9	-3.5	3.8	3.6	-3.3	-3.3
800	7.0	6.2	-5.3	-4.9	3.8	3.5	-4.9	-4.8
900	7.0	6.1	-7.1	-6.5	3.9	3.5	-7.0	-6.7
1000	7.0	6.0	-9.3	-8.6	3.9	3.4	-9.4	-8.9
1100	7.0	5.9	-12.0	-11.0	3.9	3.4	-12.3	-11.5
1200	7.0	5.8	-15.2	-13.8	4.0	3.3	-15.6	-14.4
1300	7.0	5.6	-18.9	-17.0	4.0	3.2	-19.4	-17.6
1400	7.0	5.5	-23.2	-20.7	4.0	3.1	-23.7	-21.2
1500	6.9	5.3	-28.0	-24.7	4.1	3.0	-28.5	-25.0

<sup>a</sup> See footnote *a* to Tables 1 and 2. The computed  $\kappa$  values are rather sensitive to the number of significant digits used for their determination.

for Shibata and Bartell, it is not expected that the GED experiments will show enough resolution to determine the temperature dependence of the  $r_a$ ,  $r_g$ ,  $l_g$ , and  $\kappa$  parameters of water experimentally. A particular feature of the temperature dependence of the HH and DD distances is that they go through a minimum, at about 300–400 and 900–1100 K for  $r_g$  and  $r_a$  types, respectively. It is unlikely that GED experiments will be able to confirm the latter small systematic changes. A more likely use of this information is to keep the HH and DD distances constant over a large temperature range during the GED structural analysis.

A further important conclusion of general relevance from the data presented in Table 2 is that the constrained vibrational ( $J = 0$ ) averaging does not yield correct bond length increases even over a rather large temperature interval. The  $J = 0$  averaging yields, for example, an  $r_g(\text{OH})$  distance correction of 0.000 19 Å from 0 to 800 K, while the proper rovibrational averaging yields a value an order of magnitude larger, 0.001 82 Å. It is thus very fortunate that the rotational distance corrections, due to their linear temperature dependence and independence from vibrations, can be obtained extremely simply from variational nuclear motion computations. A full quantum mechanical treatment seems unnecessary, just the linear factor in front of  $T$  must be determined through a few simple and almost cost-free low- $J$  rovibrational

computations, as verified by data presented in Table 2 and Figure 4. The factors obtained by linear fit to the variationally computed temperature-dependent  $\delta r_g$  ( $\delta r_a$ ) values, where these symbols stand for the rotational contributions to the two distance types at different temperatures, are  $2.06$  ( $2.04$ )  $\times 10^{-6}$  and  $2.02$  ( $2.00$ )  $\times 10^{-6}$  Å/K for  $\text{H}_2^{16}\text{O}$  and  $\text{D}_2^{16}\text{O}$ , respectively. The slight deviations probably reflect the precision of the data and should not be taken literally. It is also interesting to observe the behavior of the centrifugal distortion term on the HH (and DD) distance (see Figure 4). Clearly, the change over a rather large temperature range is minuscule, almost negligible, but in contrast to the bonded case, rotation results in a contraction of the nonbonding HH distance. This contraction scales linearly with the temperature, where the scaling parameter is isotopologue independent and has the same value of  $-3.6 \times 10^{-7}$  Å/K with an uncertainty of  $1 \times 10^{-7}$  Å/K for the rotational contribution to both  $r_g$  and  $r_a$ .

**4.2. Spectroscopic Parameters.** There are two important spectroscopic parameters that the present study addresses: the so-called rotational and the vibration–rotation interaction constants.

Effective rotational constants are the principal structural results obtained from fitting appropriate effective rovibrational Hamiltonians to spectroscopic data. As to computa-



TABLE 4: Vibrationally Averaged Rotational Constants, in  $\text{cm}^{-1}$ , of the  $\text{H}_2^{16}\text{O}$  Molecule up to and Including the First Decade<sup>a</sup>

<i>P</i>	<i>v</i>	<i>E<sub>v</sub></i>	$\langle A \rangle_v$		$\langle B \rangle_v$		$\langle C \rangle_v$	
			VAR	expt	VAR	expt	VAR	expt
0	(0 0 0)	4638.31	27.8656	27.8778, <sup>60</sup> 27.8787 <sup>71</sup>	14.5042	14.5092, <sup>60</sup> 14.5115 <sup>71</sup>	9.2964	9.2869, <sup>60</sup> 9.2880 <sup>71</sup>
1	(0 1 0)	1595.08	31.1105	31.1301 <sup>72</sup>	14.6658	14.6870 <sup>72</sup>	9.3565	9.1295 <sup>72</sup>
2	(0 2 0)	3152.20	35.5359	35.5867(30) <sup>61</sup>	14.8083	14.8415(24) <sup>61</sup>	9.4272	8.9745(21) <sup>61</sup>
	(1 0 0)	3657.05	27.1464	27.1221(26) <sup>61</sup>	14.2899	14.3048(23) <sup>61</sup>	9.1186	9.1046(20) <sup>61</sup>
3	(0 0 1)	3755.73	26.6402	26.6480(23) <sup>61</sup>	14.4093	14.4313(8) <sup>61</sup>	8.9835	9.1382(5) <sup>61</sup>
	(0 3 0)	4667.57	42.0170	42.132(22) <sup>62</sup>	14.9249	14.9714(59) <sup>62</sup>	9.5138	8.8350(27) <sup>62</sup>
	(1 1 0)	5235.49	30.2456	30.171(15) <sup>62</sup>	14.4629	14.4729(60) <sup>62</sup>	9.1759	8.9519(27) <sup>62</sup>
4	(0 1 1)	5331.51	29.5079	29.5226(36) <sup>62</sup>	14.5975	14.6136(15) <sup>62</sup>	9.0361	8.9931(12) <sup>62</sup>
	(0 4 0)	6135.08	52.8241		15.0023		9.6255	
	(1 2 0)	6775.96	34.4766	34.5079(5) <sup>63</sup>	14.6132	14.6332(3) <sup>63</sup>	9.2420	8.7921(3) <sup>63</sup>
	(0 2 1)	6872.15	33.3206	33.3571(3) <sup>63</sup>	14.7715	14.7817(2) <sup>63</sup>	9.0967	8.8308(1) <sup>63</sup>
5	(2 0 0)	7201.19	26.3466	26.3627(3) <sup>63</sup>	14.1044	14.1732(2) <sup>63</sup>	8.9108	8.9542(1) <sup>63</sup>
	(1 0 1)	7249.22	25.9603	25.9634(2) <sup>63</sup>	14.1977	14.1813(1) <sup>63</sup>	8.8046	8.9050(1) <sup>63</sup>
	(0 0 2)	7444.88	25.6119	25.5749(4) <sup>63</sup>	14.2758	14.2208(3) <sup>63</sup>	8.7137	9.0532(2) <sup>63</sup>
	(0 5 0)	7543.86	77.3265	73.0396 <sup>64</sup>	15.0171	15.2776 <sup>64</sup>	9.7822	8.46 <sup>64</sup>
	(1 3 0)	8275.08	41.1311	40.829(24) <sup>64</sup>	14.7367	14.7844(12) <sup>64</sup>	9.3236	8.6296(8) <sup>64</sup>
	(0 3 1)	8374.77	38.7103	38.7498(41) <sup>64</sup>	14.9293	14.9540(41) <sup>64</sup>	9.1698	8.6940(37) <sup>64</sup>
	(2 1 0)	8761.92	29.3371	29.3633(35) <sup>64</sup>	14.2950	14.2849(12) <sup>64</sup>	8.9634	8.7890(14) <sup>64</sup>
6	(1 1 1)	8807.03	28.7099	28.7528(21) <sup>64</sup>	14.3995	14.3981(8) <sup>64</sup>	8.8548	8.8212(11) <sup>64</sup>
	(0 1 2)	9000.39	28.2175	28.2152(41) <sup>64</sup>	14.4829	14.5063(9) <sup>64</sup>	8.7624	8.8581(6) <sup>64</sup>
	(0 6 0)	8872.17	169.598		14.9575		10.0315	
	(1 4 0)	9725.56	61.0866		14.8221		9.4419	
	(0 4 1)	9834.76	47.1102		15.0647		9.2622	
7	(2 2 0)	10285.09	33.3045		14.4587		9.0224	
	(1 2 1)	10329.17	32.3186		14.5798		8.9099	
	(0 2 2)	10522.47	31.6143		14.6764		8.8157	
	(3 0 0)	10598.60	25.4058		13.9737		8.6469	
	(2 0 1)	10612.12	25.2285		14.0148		8.5983	
	(1 0 2)	10868.41	25.2709		13.9850		8.6234	
	(0 0 3)	11031.94	24.5367		14.1643		8.4208	

<sup>a</sup> *P* = polyad number defined as  $P = 2n_1 + n_2 + 2n_3$ ; *v* = (*n*<sub>1</sub> *n*<sub>2</sub> *n*<sub>3</sub>), approximate normal-mode labeling of the variationally computed vibrational band origins (VBO); *E<sub>v</sub>* = wavenumber, in  $\text{cm}^{-1}$ , of the variational VBO; VAR = variationally computed expectation values, based on an exact kinetic energy operator and the purely ab initio adiabatic CVRQD PES; expt = experimental results from the literature. The underlined digits are not converged due to the fact that the *A* and *B* functions in the Eckart frame, where the reference configuration is the bent equilibrium structure, are singular at linear geometries. While the nuclear motion computations utilized nuclear masses, computation of the effective rotational constants was based on atomic masses. The reference structure chosen for the Eckart frame corresponds to the equilibrium structural parameters of the CVRQD PES and its orientation to the principal axes system with the molecule lying in the *x*–*y* plane.

tions, the direct route yields effective, strictly speaking vibrationally averaged, rotational constants as expectation values, employing vibrational wave functions from converged variational nuclear motion calculations (see eq 14). It is important to emphasize that pure vibrational wave functions for triatomic molecules can be determined with relatively little numerical effort. Note also that vibrational wave functions can also be obtained for much larger systems, perhaps up to 6–7 atoms with a complete kinetic energy operator,<sup>53,54</sup> though at a much larger expense.

Some of the vibrationally averaged computed rotational constants of low-lying states up to the second decade of  $\text{H}_2^{16}\text{O}$  and  $\text{D}_2^{16}\text{O}$ , given in Tables 4 and 5, respectively, can be compared to experimental values taken from refs 61–74. It must be noted that different treatments of the directly measured line information result in noticeably different experimental rotational constants for water. This is due to the fact that the effective rotational constants depend not only on the extent of the experimentally available line information but also on the choice of the Hamiltonian, whether Watson-type or, e.g., Padé–Borel-type Hamiltonians are employed, how many terms they include, and whether resonances, e.g., pure vibrational Fermi or Coriolis resonances, are taken into account.<sup>74</sup> These choices introduce small deviations already for the lowest vibrational states but become more and more pronounced for the higher states and especially for the *A* constants.

Sizeable deviations are expected between the variational vibrationally averaged and the experimental effective *C* rotational constants due to the approximations detailed in eqs 12–14. Furthermore, the agreement between the computed and experimental *A* and *B* constants is not expected to be perfect either, as the experimental constants contain contributions not only from vibrations but also from centrifugal distortion, electronic, and nonadiabatic effects, none of them taken into account here. Centrifugal distortion effects, though still small, are relatively large for the water molecule.<sup>71</sup> Electronic contributions, related to the rotational *g*-factors,<sup>117</sup> are usually considered to be small, they are on the order of 100–300 MHz for water,<sup>118</sup> i.e., less than  $0.01 \text{ cm}^{-1}$ . Nonadiabatic effects have not been considered explicitly either, and their contribution to rotational constants is still hard to ascertain. It is only noted here that using atomic masses in the computations of the average rotational constants corresponds to absorbing some part of the nonadiabatic effect into the adiabatic approximation. Overall, there is only one case where theory can point to possible accuracy problems with the experimental rotational constants, and that concerns the (1 0 2) state of the first decade of  $\text{D}_2^{16}\text{O}$ .

Once the vibrationally averaged rotational constants are available, one can determine, through eq 5 and linear least-squares, the vibration–rotation interaction constants of different

**TABLE 5: Vibrationally Averaged Rotational Constants, in  $\text{cm}^{-1}$ , of the  $\text{D}_2^{16}\text{O}$  Molecule up to and Including the First Decade<sup>a</sup>**

<i>P</i>	<i>v</i>	<i>E<sub>v</sub></i>	$\langle A \rangle_v$		$\langle B \rangle_v$		$\langle C \rangle_v$	
			VAR	expt	VAR	expt	VAR	expt
0	(0 0 0)	3389.96	15.4139	15.4200, <sup>65,67</sup> 15.3846 <sup>60</sup>	7.2682	7.2730, <sup>65,67</sup> 7.2716 <sup>60</sup>	4.8512	4.8453, <sup>65,67</sup> 4.8458 <sup>60</sup>
1	(0 1 0)	1178.67	16.6281	16.6340 <sup>73</sup>	7.3330	7.3387 <sup>73</sup>	4.8706	4.7897 <sup>73</sup>
2	(0 2 0)	2337.28	18.1248	18.1427(8) <sup>65</sup>	7.3923	7.4017(7) <sup>65</sup>	4.8917	4.7341(2) <sup>65</sup>
	(1 0 0)	2671.36	15.1859	15.1801(6) <sup>65</sup>	7.1779	7.1802(7) <sup>65</sup>	4.7852	4.7800(3) <sup>65</sup>
3	(0 0 1)	2787.31	14.8831	14.8870(4) <sup>65</sup>	7.2389	7.2452(1) <sup>65</sup>	4.7351	4.7926(2) <sup>65</sup>
	(0 3 0)	3474.84	20.0255	20.0336(1), <sup>66</sup> 20.0523(20) <sup>67</sup>	7.4455	7.45376(3), <sup>66</sup> 7.4503(9) <sup>67</sup>	4.9153	4.67916(2), <sup>66</sup> 4.6875(13) <sup>67</sup>
	(1 1 0)	3841.52	16.3767	16.3644(18) <sup>67</sup>	7.2472	7.2570(9) <sup>67</sup>	4.8046	4.7145(13) <sup>67</sup>
	(0 1 1)	3955.96	15.9864	15.9899(1) <sup>67</sup>	7.3107	7.3179 <sup>67</sup>	4.7527	4.7391 <sup>67</sup>
4	(0 4 0)	4589.89	22.5314	22.5728(9) <sup>68</sup>	7.4912	7.52 <sup>68</sup>	4.9423	4.63 <sup>68</sup>
	(1 2 0)	4991.18	17.8390	17.8047(4) <sup>68</sup>	7.3090	7.3144(3) <sup>68</sup>	4.8252	4.6639(3) <sup>68</sup>
	(0 2 1)	5105.59	17.3271	17.3237(4) <sup>68</sup>	7.3774	7.3822(7) <sup>68</sup>	4.7716	4.6823(6) <sup>68</sup>
	(2 0 0)	5291.01	14.9443	14.9726(8) <sup>68</sup>	7.0925	7.1266(8) <sup>68</sup>	4.7162	4.7070(8) <sup>68</sup>
	(1 0 1)	5373.01	14.6634	14.6718(5) <sup>68</sup>	7.1498	7.1630(8) <sup>68</sup>	4.6687	4.7279(6) <sup>68</sup>
	(0 0 2)	5528.76	14.4030	14.3682(8) <sup>68</sup>	7.2026	7.1902(8) <sup>68</sup>	4.6254	4.7498(7) <sup>68</sup>
	(0 5 0)	5680.29	26.0088		7.5270		4.9742	
5	(1 3 0)	6119.54	19.6986	19.6994(4) <sup>69</sup>	7.3636	7.3696(2) <sup>69</sup>	4.8478	4.6157(3) <sup>69</sup>
	(0 3 1)	6235.46	19.0030	19.0159(4) <sup>69</sup>	7.4393	7.4428(2) <sup>69</sup>	4.7924	4.6249(3) <sup>69</sup>
	(2 1 0)	6452.74	16.1119	16.1201(3) <sup>69</sup>	7.1672	7.1698(1) <sup>69</sup>	4.7357	4.6659(4) <sup>69</sup>
	(1 1 1)	6532.78	15.7510	15.7615(3) <sup>69</sup>	7.2272	7.2293(1) <sup>69</sup>	4.6866	4.6727(7) <sup>69</sup>
	(0 1 2)	6686.65	15.4141	15.4158(3) <sup>69</sup>	7.2806	7.2877(2) <sup>69</sup>	4.6417	4.6790(5) <sup>69</sup>
	(0 6 0)	6742.90	31.2393		7.5493		5.0131	
	(1 4 0)	7225.23	22.1813		7.4098		4.8738	
	(0 4 1)	7344.43	21.1694		7.4957		4.8161	
	(2 2 0)	7593.37	17.5369	17.4564(108) <sup>70</sup>	7.2315	7.2537(45) <sup>70</sup>	4.7554	4.6333(70) <sup>70</sup>
	(1 2 1)	7672.80	17.0597	17.0486(10) <sup>70</sup>	7.2963	7.3125(3) <sup>70</sup>	4.7048	4.6065(2) <sup>70</sup>
6	(0 2 2)	7826.27	16.6189	16.8579(32) <sup>70</sup>	7.3522	7.2921(69) <sup>70</sup>	4.6585	4.6991(58) <sup>70</sup>
	(3 0 0)	7851.63	14.6674	14.3544(338) <sup>70</sup>	7.0205	6.9561(70) <sup>70</sup>	4.6387	4.6133(39) <sup>70</sup>
	(2 0 1)	7898.31	14.4246	14.3006(164) <sup>70</sup>	7.0686	7.1127(27) <sup>70</sup>	4.5976	4.6195(31) <sup>70</sup>
	(1 0 2)	8052.91	14.2612	14.5518(301) <sup>70</sup>	7.0995	7.1866(49) <sup>70</sup>	4.5715	4.7439(55) <sup>70</sup>
	(0 0 3)	8219.17	13.9425	14.0405(163) <sup>70</sup>	7.1654	7.1667(27) <sup>70</sup>	4.5174	4.6732(58) <sup>70</sup>

<sup>a</sup> See footnote *a* to Table 4.**TABLE 6: Low-Order Vibration–Rotation Interaction Constants (Eq 5), in  $\text{cm}^{-1}$ , the  $\text{H}_2^{16}\text{O}$  Molecule<sup>a</sup>**

const	expt <sup>60</sup>	VPT2 <sup>119</sup>	VAR1	VAR2	VAR3	VAR4
$\alpha_1^A$	0.750	0.685	0.719	0.941(353)	0.880(117)	0.417(151)
$\alpha_2^A$	−2.941	−2.617	−3.245	−3.618(188)	−3.466(119)	−2.516(129)
$\alpha_3^A$	1.253	1.159	1.225	1.447(353)	1.306(119)	1.176(152)
$\alpha_1^B$	0.238	0.221	0.214	0.213(5)	0.197(7)	0.259(29)
$\alpha_2^B$	−0.160	−0.156	−0.162	−0.154(3)	−0.179(7)	−0.145(25)
$\alpha_3^B$	0.078	0.099	0.095	0.094(5)	0.117(7)	0.056(29)
$\alpha_1^C$	0.202	0.177	0.178	0.181(3)	0.200(6)	
$\alpha_2^C$	0.139	0.147	−0.060	−0.063(2)	−0.051(6)	
$\alpha_3^C$	0.145	0.143	0.313	0.316(3)	0.287(6)	
$\gamma_{11}^A; \gamma_{11}^B$						−0.078(39); 0.021(7)
$\gamma_{12}^A; \gamma_{12}^B$						−0.283(64); 0.027(12)
$\gamma_{13}^A; \gamma_{13}^B$						0.095(56); −0.021(11)
$\gamma_{22}^A; \gamma_{22}^B$						0.556(35); −0.004(7)
$\gamma_{23}^A; \gamma_{23}^B$						−0.404(41); 0.020(8)
$\gamma_{33}^A; \gamma_{33}^B$						0.067(38); −0.016(7)

<sup>a</sup> Expt = experiment; VPT2 = vibrational perturbation theory carried out to second order; VAR1 = results based on the inversion of the information contained in the variationally determined effective rotational constants of the (0 0 0), (0 1 0), (1 0 0), and (0 0 1) vibrational states; VAR2 = results based on a least-squares fit of  $\alpha$  constants including all variationally determined effective rotational constants corresponding to *P* = 0, 1, and 2; VAR3 = results based on a least-squares fit of  $\alpha$  constants against variationally determined effective rotational constants reported in Table 4 (altogether 20 states are employed, all those for which all three rotational constants are fully converged); VAR4 = results based on a least-squares fit of  $\alpha$  and  $\gamma$  constants against variationally determined effective rotational constants reported in Table 4 (altogether 20 states are employed, all those for which all three rotational constants are fully converged). In the VAR2, VAR3, and VAR4 fittings the equilibrium rotational constants were fixed at their CVRQD values,  $A_e = 27.3853$ ,  $B_e = 14.5805$ , and  $C_e = 9.5148 \text{ cm}^{-1}$ , and the resulting standard errors are given in parentheses. As expected, the root-mean-square error, in  $\text{cm}^{-1}$ , of the VAR3 fit, {0.601, 0.037} for {*A*, *B*} decreases to {0.118, 0.023} for VAR4.

order. Here only the constants referring to the *A* and *B* rotational constants are considered.

For prototypical semirigid molecules, for which there is at least 2 orders of magnitude difference between vibration–rotation interaction constants of consecutive order, the lowest-order

vibration–rotation interaction constants can be computed straightforwardly from the vibrationally averaged rotational constants of the lowest vibrational states. The simplest approach to determine the three  $\alpha^B$  constants of water, for example, assumes that all higher-order constants are zero and uses the following four averaged

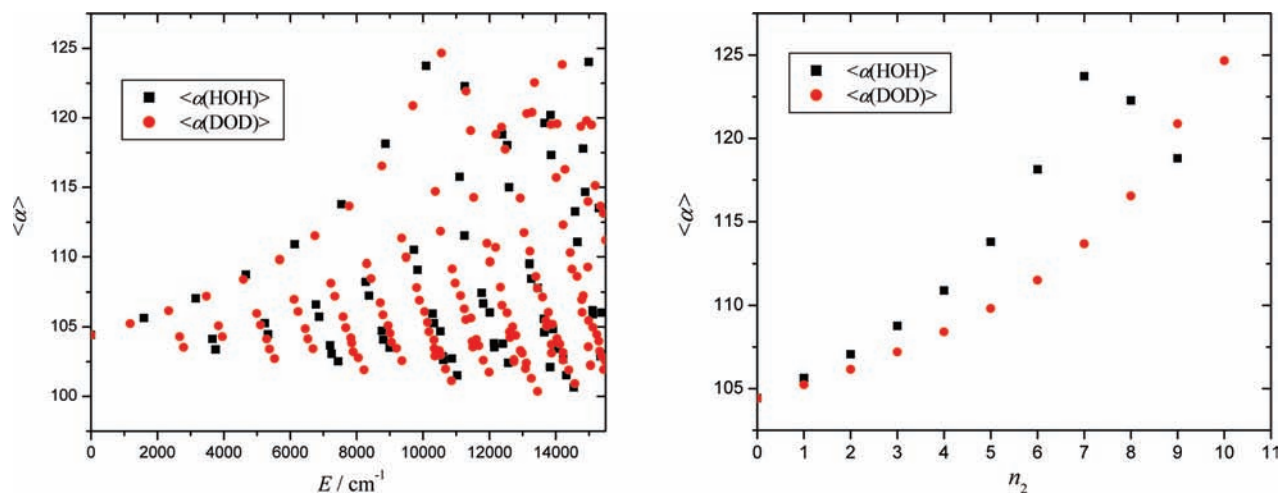


**Figure 1.** Variationally computed expectation values of the bond angles of  $\text{H}_2^{16}\text{O}$  and  $\text{D}_2^{16}\text{O}$  as a function of the vibrational band origins (left) and the bending vibrational states ( $0\ n_2\ 0$ ) (right). The energies are relative to the zero-point levels, i.e., 4638 and 3390  $\text{cm}^{-1}$  for  $\text{H}_2^{16}\text{O}$  and  $\text{D}_2^{16}\text{O}$ , respectively. On the left panel all the vibrational states are shown up to 15 500  $\text{cm}^{-1}$ .

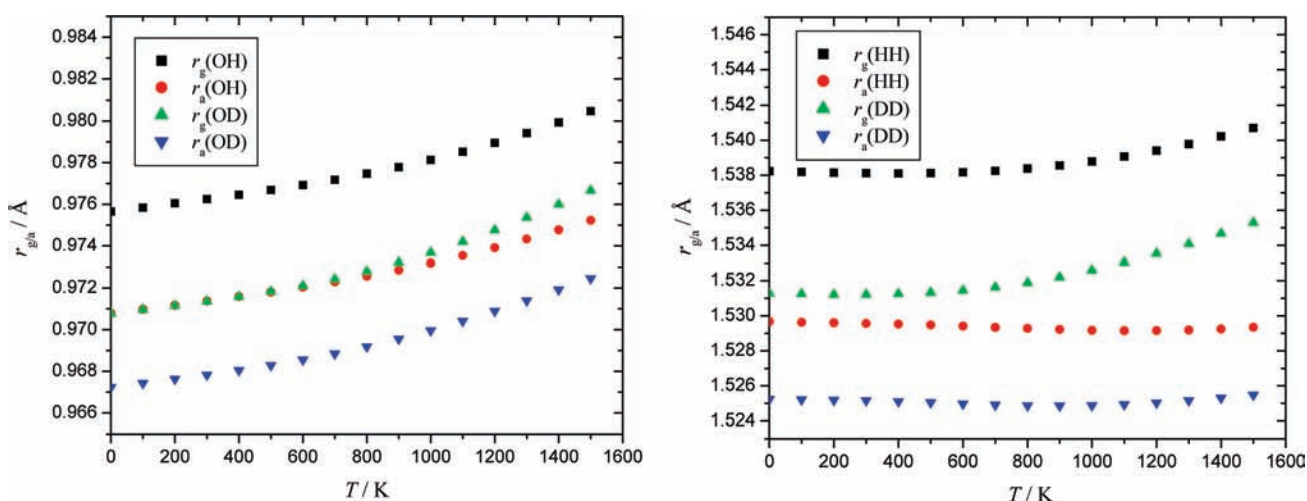


**Figure 2.** Temperature dependence of the length of the average internuclear ( $r_{\text{g}}$ ) and inverse internuclear ( $r_{\text{a}}$ ) bonded and nonbonded distances of the  $\text{H}_2^{16}\text{O}$  and  $\text{D}_2^{16}\text{O}$  molecules computed variationally using all rotational–vibrational states populated significantly at a given temperature  $T$ .

rotational constants:  $B_{000}$ ,  $B_{100}$ ,  $B_{010}$ , and  $B_{001}$ . The  $\alpha$  constants computed this way (see the VARI results of Table 6) agree reasonably well with the experimental and VPT2 values of previous studies.<sup>119</sup> Nevertheless, deviations on the order of 10% are not uncommon.

Use of the many average rotational constants determined in this study yields information also on the  $\gamma$  constants and even higher-order vibration–rotation parameters could be determined. The  $\gamma$  constants of water have never been determined before. From many tests performed during least-squares fitting it became clear that the vibration–rotation interaction constants, depending on the use of more or less variationally computed rotational constants, can take values in a rather substantial range. Some of these results are detailed in Table 6. Clearly, for water, for which differences between the  $\mathbf{B}$ ,  $\alpha$ , and  $\gamma$  constants are often less than 10-fold, the least-squares procedure does not result in unique low-order vibration–rotation interaction constants.

## 5. Conclusions

In some influential publications and related lectures, Richards<sup>120</sup> and then Schaefer<sup>121,122</sup> categorized the development of computational quantum chemistry into three ages. Within this scheme, quantum chemistry was basically identified, as it is still usually done, with electronic structure theory and thus only the

developments of electronic structure theory were considered when the successes of quantum chemistry were discussed. Then, the year 1970 was chosen as the start of the third age of quantum chemistry whereby theory, again, electronic structure theory, has become able to make quantitative predictions and thus challenge (or even overrule) experiments or their interpretation. Of course, the other important branch of quantum chemistry deals with the motion of the nuclei within the molecule, observed through molecular (vibration–rotation) spectra or the realization of chemical reactions. While electronic structure theory has been quite successful in yielding quantities which can be related, usually at an elementary level, to experimental observables, quantitative agreement with experiments can only be expected when the motions of the nuclei are also considered. It is hoped in this context that the fourth age of quantum chemistry will arrive soon, whereby quantum chemistry would quantitatively bridge the gap between “effective”, experimental observables and “equilibrium” computed quantities at even elevated temperatures of interest.

This study, with the help of state-of-the-art, third-age electronic structure theory together with variational nuclear motion computations, constitutes a step toward fourth-age methodology by computing thermally averaged structural and vibrationally averaged spectroscopic constants for two iso-

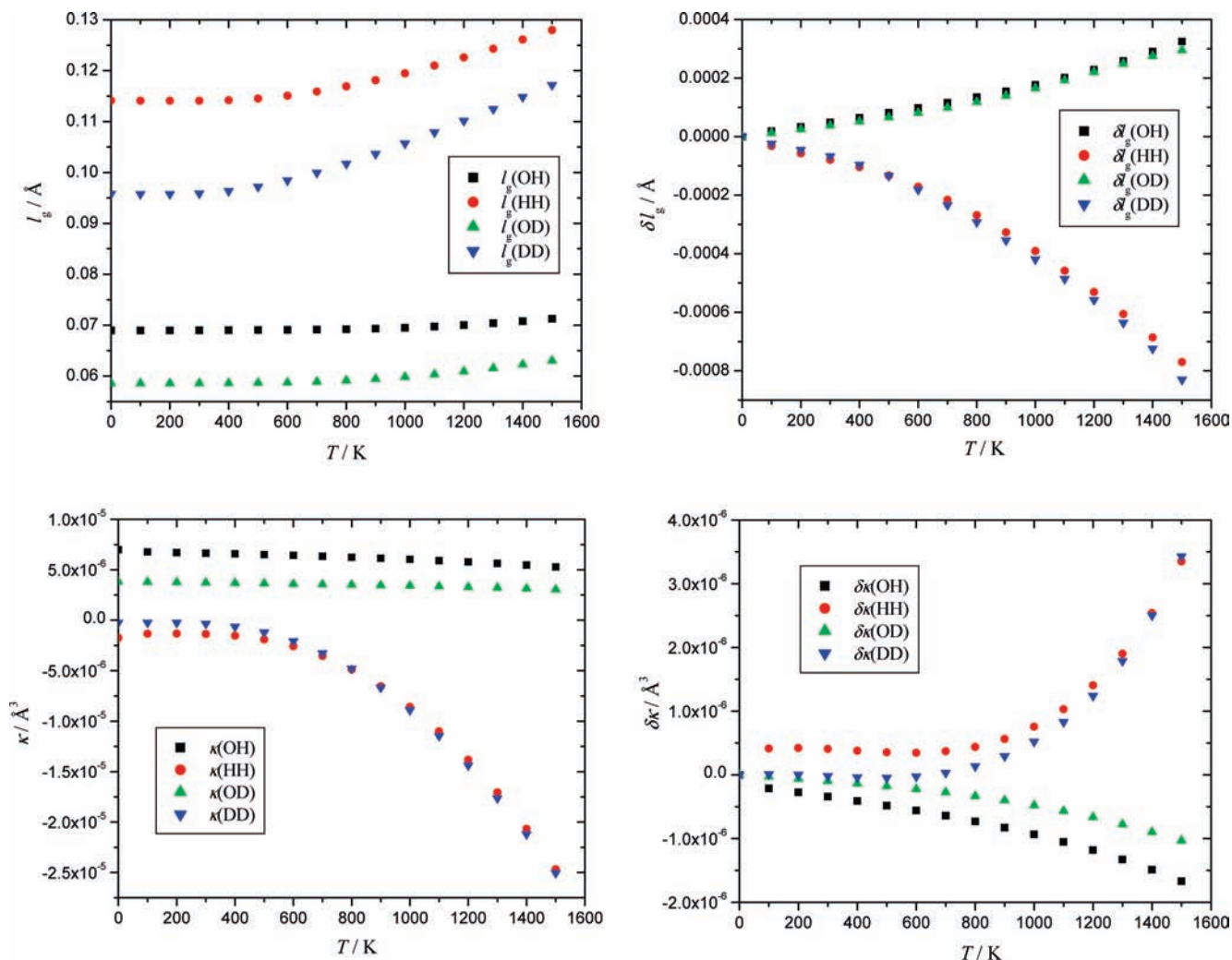


**Figure 3.** Temperature dependence of the rms amplitude ( $l_g$ ) and the anharmonicity ( $\kappa$ ) parameters (left panel) and the rotational contributions to them (right panel) for  $\text{H}_2^{16}\text{O}$  and  $\text{D}_2^{16}\text{O}$ .

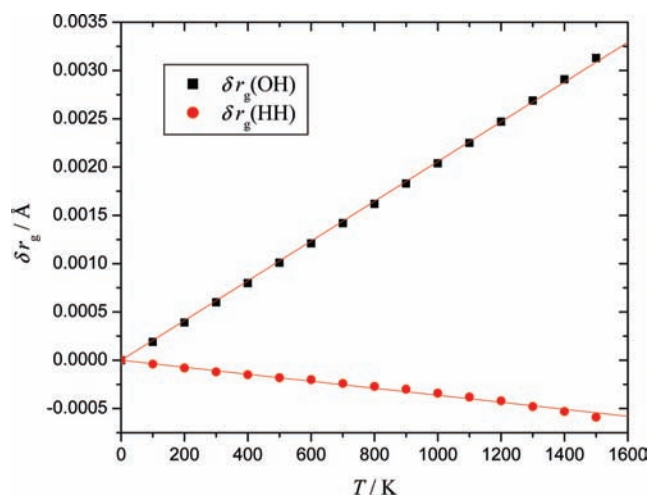


**Figure 4.** Temperature dependence of the rotational contributions to the  $r_g(\text{OH})$  and  $r_g(\text{HH})$  parameters of  $\text{H}_2^{16}\text{O}$ . The linear fits,  $\delta r_g = \sigma T$ , gave  $\sigma$  parameters of  $2.06 \times 10^{-6}$  and  $-3.6 \times 10^{-7}$  Å/K for  $\delta r_g(\text{OH})$  and  $\delta r_g(\text{HH})$ , respectively.

pologues of the water molecule,  $\text{H}_2^{16}\text{O}$  and  $\text{D}_2^{16}\text{O}$ . The usually fully converged variational nuclear motion computations involved exact kinetic energy operators and the high-quality adiabatic CVRQD PESs. The most important results of this study can be summarized as follows:

(1) The structural quantities computed include several different vibrational averages. As suggested by simple perturbative arguments and confirmed here variationally, the order of the distances is  $\langle r^3 \rangle^{1/3} > \langle r^2 \rangle^{1/2} > \langle r \rangle > \langle r^{-1} \rangle^{-1} > \langle r^{-2} \rangle^{-1/2} > \langle r^{-3} \rangle^{-1/3} > r_e$ . Other simple PT formulas, like  $\langle x \rangle = 3/2 a \langle x^2 \rangle$  and  $r_a = r_g - l_g^2/r$ , where  $x = r - r_e$  and  $l_g^2 = \langle x^2 \rangle - \langle x \rangle^2$ , have also been confirmed. One of the most remarkable variations among the computed structural parameters upon excitation is that of the average bond angle, which shows a very regular behavior and starts decreasing for excitation energies beyond the barrier to linearity (see Figure 1).

(2) Precise structural data, including average internuclear ( $r_g$ ) and inverse internuclear ( $r_a$ ) distances, root-mean-square (rms) amplitudes ( $l_g$ ), and  $\kappa$  anharmonicity parameters, all usually refined in GED structural analyses, have been determined in the temperature range of 0–1500 K for the water isotopologues  $\text{H}_2^{16}\text{O}$  and  $\text{D}_2^{16}\text{O}$ . The values obtained show excellent agreement with most results from an old GED experiment performed at 302 K but are expected to be considerably more accurate. While it would be nice if in the future GED could be used to check the validity of the structural parameters derived here over the whole temperature range, this is not expected due to the low scattering power of the H (and D) atoms. Of course, the same procedure applied here to water can straightforwardly be extended to larger systems and should supplement problematic GED experiments, especially at higher temperatures.



(3) Constrained vibrational ( $J = 0$ ) averaging does not yield correct bond length increases even over a rather large temperature range. The distance corrections due to rotations are substantial but turn out to be linearly dependent on  $T$ , as suggested by classical mechanics. Thus, the centrifugal distortion correction can be treated perfectly well through a few simple computations as only the linear factor in front of  $T$  needs to be determined. These factors appear to be isotope independent and positive and negative for the bonded (OH/OD) and nonbonded (HH/DD) distances, respectively.

(4) General formulas have been derived, allowing the determination of vibrationally averaged rotational constants referring to the Eckart frame used by experimental spectroscopists for molecules of arbitrary size. The simplifications yielding such effective rotational constants are given clearly and explicitly. In general, these vibrationally averaged rotational constants are not the same as the effective rotational constants determined by spectroscopists fitting effective Hamiltonians to rotational line information. A small part of the difference, on the order of  $0.01\text{--}0.05\text{ cm}^{-1}$ , comes from the neglect of certain rotational, electronic, and nonadiabatic effects. The most important part, however, comes from the neglect of terms in the effective rotational Hamiltonian derived for a given vibrational state. It is expected that a closer correspondence between variational and spectroscopic effective spectroscopic constants can be worked out in the near future. As to water, the shortcomings of the present theoretical treatment affect the comparison for the  $C$  but not for the  $A$  and  $B$  rotational constants between experiment and theory. Indeed, we found nice agreement for the latter two sets of constants referring to in-plane axes for all the states investigated. Apart from the purely bending states, the average deviation between the vibrationally averaged and the experimental effective rotational constants is just a few  $0.01\text{ cm}^{-1}$ .

(5) The fact that rotational constants can be derived for a large number of vibrational states variationally opens a way to determine vibration–rotation interaction constants of different order variationally. It is expected that once perturbative formulas will be used to determine not only so-called  $\alpha$  but also  $\gamma$  constants, this possibility for comparison should prove illuminating. As to water, it is clear that the usually required 2 orders of magnitude difference in the rotational and vibration–rotation constants does not hold. Thus, while this study yielded the first set of  $\gamma$  constants for  $\text{H}_2^{16}\text{O}$ , the vibration–rotation constants can not be determined uniquely and precisely as their values depend strongly on the number and quality of information used during their determination.

**Acknowledgment.** The work performed received support from the Hungarian Scientific Research Fund, OTKA, through grant K72885. Discussions with Drs. Jean Demaison (Lille, France), Ken Hedberg (Corvallis, U.S.A.), Jeremy Hutson (Durham, U.K.), and Olga Naumenko (Tomsk, Russia) on certain aspects of this article are gratefully acknowledged.

## References and Notes

- Wang, X. G.; Sibert, E. L. *J. Chem. Phys.* **2000**, *113*, 5384.
- Schuurman, M. S.; Allen, W. D.; Schaefer, H. F., III. *J. Comput. Chem.* **2005**, *26*, 1106.
- Nielsen, H. H. *Rev. Mod. Phys.* **1951**, *23*, 90.
- Mills, I. M. In *Molecular Spectroscopy: Modern Research*; Rao, K. N., Mathews, C. W., Eds.; Academic Press: New York, 1972.
- Gaw, J. F.; Willetts, A.; Green, W. H.; Handy, N. C. *Advances in Molecular Vibrations and Collision Dynamics*; JAI Press: Greenwich, CT, 1990.
- Clabo, D. A.; Allen, W. D.; Yamaguchi, Y.; Remington, R. B.; Schaefer, H. F., III. *Chem. Phys.* **1988**, *123*, 187.
- Allen, W. D.; Yamaguchi, Y.; Császár, A. G.; Clabo, D. A.; Remington, R. B.; Schaefer, H. F., III. *Chem. Phys.* **1990**, *145*, 427.
- Willetts, A.; Handy, N. C.; Green, W. H.; Jayatilaka, D. *J. Phys. Chem.* **1990**, *94*, 5608.
- Aliev, M. R.; Watson, J. K. G. In *Molecular Spectroscopy: Modern Research*; Narahari Rao, K., Ed.; Academic Press: San Diego, CA, 1985; Vol. III, pp 1–67.
- Wang, X.-G.; Carrington, T., Jr. *J. Chem. Phys.* **2008**, *129*, 234102.
- Stanton, J. F. *J. Chem. Phys.* **2007**, *126*, 134309.
- Oka, T. *Rev. Mod. Phys.* **1992**, *64*, 1141.
- Tennyson, J.; Sutcliffe, B. T. *Mol. Phys.* **1984**, *51*, 887.
- Polyansky, O. L. *J. Mol. Spectrosc.* **1985**, *112*, 79.
- Bernath, P. F. *Phys. Chem. Chem. Phys.* **2002**, *4*, 1501.
- Morse, P. *Phys. Rev.* **1929**, *34*, 57.
- Iwasaki, M.; Hedberg, K. *J. Chem. Phys.* **1962**, *36*, 2961.
- Eckart, C. *Phys. Rev.* **1935**, *47*, 552.
- Wilson, E. B.; Howard, L. S. *J. Chem. Phys.* **1936**, *4*, 260.
- Reitan, A. *Acta Chem. Scand.* **1958**, *12*, 785.
- Morino, Y.; Nakamura, J.; Moore, P. W. *J. Chem. Phys.* **1962**, *36*, 1050.
- Toyama, M.; Oka, T.; Morino, Y. *J. Mol. Spectrosc.* **1964**, *13*, 193.
- Kuchitsu, K. *Bull. Chem. Soc. Jpn.* **1967**, *40*, 505.
- Kuchitsu, K.; Bartell, L. S. *J. Chem. Phys.* **1962**, *36*, 2460.
- Kuchitsu, K.; Bartell, L. S. *J. Chem. Phys.* **1961**, *35*, 1945.
- Nakata, M.; Kuchitsu, K.; Mills, I. M. *J. Phys. Chem.* **1984**, *88*, 344.
- Bartell, L. S. *J. Chem. Phys.* **1955**, *23*, 1219.
- Bartell, L. S.; Kuchitsu, K.; de Neui, R. J. *J. Chem. Phys.* **1961**, *135*, 1211.
- Bartell, L. S. *J. Chem. Phys.* **1963**, *38*, 1827.
- Bartell, L. S. *J. Chem. Phys.* **1979**, *70*, 4581.
- Bartell, L. S. *J. Phys. Chem.* **1985**, *89*, 2540.
- Stanton, J. F.; Bartell, L. S. *J. Chem. Phys.* **1985**, *89*, 2544.
- Herschbach, D. R.; Laurie, V. W. *J. Chem. Phys.* **1962**, *37*, 1668.
- Laurie, V. W.; Herschbach, D. R. *J. Chem. Phys.* **1962**, *37*, 1687.
- Mills, I. M. *J. Phys. Chem.* **1976**, *80*, 1189.
- Watson, J. K. G. *J. Mol. Spectrosc.* **1973**, *48*, 479.
- Smith, J. G.; Watson, J. K. G. *J. Mol. Spectrosc.* **1978**, *69*, 47.
- Watson, J. K. G.; Roytberg, A.; Ulrich, W. *J. Mol. Spectrosc.* **1999**, *196*, 102.
- Bonham, R. A.; Su, L. S. *J. Chem. Phys.* **1966**, *45*, 2827.
- Spiridonov, V. P. *J. Mol. Struct.* **1995**, *346*, 131.
- Spiridonov, V. P.; Tarasov, Yu. I.; Novosadov, B. K.; Nikitin, O. Yu.; Maslov, I. V. *J. Mol. Struct.* **1997**, *413–414*, 463.
- Hinchley, S. L.; Wann, D. A.; Rankin, D. W. H. *Int. J. Quantum Chem.* **2005**, *101*, 878.
- Demaison, J.; Császár, A. G.; Dehayem-Kamadjeu, A. *J. Phys. Chem. A* **2006**, *110*, 13609.
- Kuchitsu, K.; Nakata, M.; Yamamoto, S. In *Stereochemical Applications of Gas-Phase Electron Diffraction, Part A*; Hargittai, I., Hargittai, M., Eds.; VCH: New York, 1988.
- Pulay, P.; Meyer, W.; Boggs, J. E. *J. Chem. Phys.* **1978**, *68*, 5077.
- Kasalová, V.; Allen, W. D.; Schaefer, H. F.; Czinki, E.; Császár, A. G. *J. Comput. Chem.* **2007**, *28*, 1373.
- Allen, W. D.; Czinki, E.; Császár, A. G. *Chem.—Eur. J.* **2004**, *10*, 4512.
- Demaison, J. *Mol. Phys.* **2007**, *105*, 3109.
- Polyansky, O. L.; Császár, A. G.; Shirin, S. V.; Zobov, N. F.; Barletta, P.; Tennyson, J.; Schwenke, D. W.; Knowles, P. J. *Science* **2003**, *299*, 539.
- Császár, A. G.; Tarczay, G.; Leininger, M. L.; Polyansky, O. L.; Tennyson, J.; Allen, W. D. In *Spectroscopy from Space*; Demaison, J., Sarka, K., Cohen, E. A., Eds.; Kluwer: Dordrecht, The Netherlands, 2001; pp 317–339.
- Barletta, P.; Shirin, S. V.; Zobov, N. F.; Polyansky, O. L.; Tennyson, J.; Valeev, E. F.; Császár, A. G. *J. Chem. Phys.* **2006**, *125*, 204307.
- Császár, A. G.; Czakó, G.; Furtenbacher, T.; Tennyson, J.; Szalay, V.; Shirin, S. V.; Zobov, N. F.; Polyansky, O. L. *J. Chem. Phys.* **2005**, *122*, 214305.
- (a) Mátyus, E.; Czakó, G.; Sutcliffe, B. T.; Császár, A. G. *J. Chem. Phys.* **2007**, *127*, 084102. (b) Mátyus, E.; Šimunek, J.; Császár, A. G. *J. Chem. Phys.*, DOI: 10.1063/1.3187528.
- Mátyus, E.; Czakó, G.; Császár, A. G. *J. Chem. Phys.* **2009**, *130*, 134112.
- Yurchenko, S. N.; Zheng, J.; Thiel, W.; Carvajal, M.; Lin, H.; Jensen, P. In *Remote Sensing of the Atmosphere for Environment Security*; Perrin, A., Ed.; Springer: Dordrecht, The Netherlands, 2006; pp 171–183.
- Yurchenko, S. N.; Thiel, W.; Jensen, P. *J. Mol. Spectrosc.* **2007**, *245*, 126.

- (57) Shirin, S. V.; Polyansky, O. L.; Zobov, N. F.; Ovsyannikov, R. I.; Császár, A. G.; Tennyson, J. *J. Mol. Spectrosc.* **2006**, *236*, 216.
- (58) Mecke, R.; Baumann, W.; Freudenburg, K. *Z. Phys.* **1933**, *81*, 313, 445, 465.
- (59) Darling, B. T.; Dennison, D. M. *Phys. Rev.* **1940**, *57*, 128.
- (60) Benedict, W. S.; Gailar, N.; Plyler, E. K. *J. Chem. Phys.* **1956**, *24*, 1139.
- (61) Flaud, J.-M.; Camy-Peyret, C. *J. Mol. Spectrosc.* **1974**, *51*, 142.
- (62) Camy-Peyret, C.; Flaud, J.-M. *J. Mol. Spectrosc.* **1976**, *59*, 327.
- (63) Kwan, Y. Y. *J. Mol. Spectrosc.* **1978**, *71*, 260.
- (64) Ulenikov, O. N.; Ushakova, G. A. *J. Mol. Spectrosc.* **1986**, *117*, 195.
- (65) Papineau, N.; Flaud, J.-M.; Camy-Peyret, C.; Guelachvili, G. *J. Mol. Spectrosc.* **1981**, *87*, 219.
- (66) Bykov, A.; Naumenko, O.; Sinita, L.; Voronin, B.; Winnewisser, B. P. *J. Mol. Spectrosc.* **2000**, *199*, 158.
- (67) He, S.-G.; Ulenikov, O. N.; Onopenko, G. A.; Bekhtereva, E. S.; Wang, X.-H.; Hu, S.-M.; Lin, H.; Zhu, Q.-S. *J. Mol. Spectrosc.* **2000**, *200*, 34.
- (68) Wang, X.-H.; Ulenikov, O. N.; Onopenko, G. A.; Bekhtereva, E. S.; He, S.-G.; Hu, S.-M.; Lin, H.; Zhu, Q.-S. *J. Mol. Spectrosc.* **2000**, *200*, 25.
- (69) Ormsby, P. S.; Narahari Rao, K.; Winnewisser, M.; Winnewisser, B. P.; Naumenko, O. V.; Bykov, A. D.; Sinita, L. N. *J. Mol. Spectrosc.* **1993**, *158*, 109.
- (70) Ulenikov, O. N.; He, S.-G.; Onopenko, G. A.; Bekhtereva, E. S.; Wang, X.-H.; Hu, S.-M.; Lin, H.; Zhu, Q.-S. *J. Mol. Spectrosc.* **2000**, *204*, 216.
- (71) De Lucia, F. C.; Helminger, P.; Cook, R. L.; Gordy, W. *Phys. Rev. A* **1972**, *5*, 487.
- (72) Toth, R. A. *J. Opt. Soc. Am. B* **1991**, *8*, 2236.
- (73) Messer, J. K.; De Lucia, F. C.; Helminger, P. *J. Mol. Spectrosc.* **1984**, *105*, 139.
- (74) Flaud, J.-M.; Camy-Peyret, C.; Bykov, A.; Naumenko, O.; Petrova, T.; Scherbakov, A.; Sinita, L. *J. Mol. Spectrosc.* **1997**, *183*, 300.
- (75) Shibata, S.; Bartell, L. S. *J. Chem. Phys.* **1965**, *42*, 1147.
- (76) Mawhorter, R. J.; Fink, M.; Archer, B. T. *J. Chem. Phys.* **1983**, *79*, 170.
- (77) Mawhorter, R. J.; Fink, M. *J. Chem. Phys.* **1983**, *79*, 3292.
- (78) Miller, B. R.; Fink, M. *J. Chem. Phys.* **1985**, *83*, 939.
- (79) Hilderbrandt, R. L.; Kohl, D. A. *J. Mol. Struct. (THEOCHEM)* **1981**, *85*, 25.
- (80) Kohl, D. A.; Hilderbrandt, R. L. *J. Mol. Struct. (THEOCHEM)* **1981**, *85*, 325.
- (81) Császár, A. G.; Allen, W. D.; Schaefer, H. F. *J. Chem. Phys.* **1998**, *108*, 9751.
- (82) Allen, W. D.; East, A. L. L.; Császár, A. G. In *Structures and Conformations of Non-Rigid Molecules*; Laane, J., Dakkouri, M., van der Veken, B., Oberhammer, H., Eds.; Kluwer: Dordrecht, The Netherlands, 1993; p 343.
- (83) Császár, A. G.; Kain, J. S.; Polyansky, O. L.; Zobov, N. F.; Tennyson, J. *Chem. Phys. Lett.* **1998**, *293*, 317. **1999**, *312*, 613 (E).
- (84) Quiney, H. M.; Barletta, P.; Tarczay, G.; Császár, A. G.; Polyansky, O. L.; Tennyson, J. *Chem. Phys. Lett.* **2001**, *344*, 413.
- (85) Pyykkö, P.; Dyal, K.; Császár, A. G.; Tarczay, G.; Polyansky, O. L.; Tennyson, J. *Phys. Rev. A* **2001**, *63*, 4502.
- (86) Schwenke, D. W. *J. Chem. Phys.* **2003**, *118*, 6898.
- (87) Czakó, G.; Furtenbacher, T.; Császár, A. G.; Szalay, V. *Mol. Phys.* **2004**, *102*, 2411.
- (88) Furtenbacher, T.; Czakó, G.; Sutcliffe, B. T.; Császár, A. G.; Szalay, V. *J. Mol. Struct.* **2006**, *780–781*, 283.
- (89) Jacobi, C. G. *J. Cr. Hebd. Acad. Sci.* **1842**, *15*, 236.
- (90) Radau, R. *Ann. Sci. Ecole Norm. S.* **1868**, *5*, 311.
- (91) Makarewicz, J. *J. Phys. B* **1988**, *21*, 1803.
- (92) Sutcliffe, B. T.; Tennyson, J. *Int. J. Quantum Chem.* **1991**, *39*, 183.
- (93) Harris, D. O.; Engerholm, G. G.; Gwinn, W. D. *J. Chem. Phys.* **1965**, *43*, 151.
- (94) Dickinson, A. S.; Certain, P. R. *J. Chem. Phys.* **1968**, *49*, 4209.
- (95) Light, J. C.; Hamilton, I. P.; Lill, J. V. *J. Chem. Phys.* **1985**, *82*, 1400.
- (96) Bačić, Z.; Light, J. C. *Annu. Rev. Phys. Chem.* **1989**, *40*, 469.
- (97) Szalay, V. *J. Chem. Phys.* **1993**, *99*, 1978.
- (98) Szalay, V. *J. Chem. Phys.* **1996**, *105*, 6940.
- (99) Light, J. C.; Carrington, T., Jr. *Adv. Chem. Phys.* **2000**, *114*, 263.
- (100) Szalay, V.; Czakó, G.; Nagy, Á.; Furtenbacher, T.; Császár, A. G. *J. Chem. Phys.* **2003**, *119*, 10512.
- (101) Lanczos, C. *J. Res. Natl. Bur. Stand.* **1950**, *45*, 255.
- (102) Kraitchman, J. *Am. J. Phys.* **1953**, *21*, 17.
- (103) Costain, C. C. *J. Chem. Phys.* **1958**, *29*, 864.
- (104) Demaison, J.; Rudolph, H. D. *J. Mol. Spectrosc.* **2002**, *215*, 78.
- (105) Cook, R. L.; De Lucia, F. C.; Helminger, P. *J. Mol. Spectrosc.* **1974**, *53*, 62.
- (106) Vázquez, J.; Stanton, J. F. Personal communication, 2008.
- (107) Watson, J. K. G. *J. Chem. Phys.* **1967**, *46*, 1935.
- (108) Lukka, T. J.; Kauppi, E. *J. Chem. Phys.* **1995**, *103*, 6586.
- (109) Littlejohn, R. G.; Reinsch, M. *Rev. Mod. Phys.* **1997**, *69*, 213.
- (110) Watson, J. K. G. *Mol. Phys.* **1968**, *15*, 479.
- (111) Ernesti, A.; Hutson, J. M. *Chem. Phys. Lett.* **1994**, *222*, 257.
- (112) Tennyson, J.; Bernath, P. F.; Brown, L. R.; Campargue, A.; Carleer, M. R.; Császár, A. G.; Gamache, R. R.; Hodges, J. T.; Jenouvrier, A.; Naumenko, O. V.; Polyansky, O. L.; Rothman, L. S.; Toth, R. A.; Vandaele, A. C.; Zobov, N. F.; Daumont, L.; Fazliev, A. Z.; Furtenbacher, T.; Gordon, I. F.; Mikhailenko, S. N.; Shirin, S. V. *J. Quantum Spectrosc. Radiat. Transfer* **2009**, *110*, 573.
- (113) Shirin, S. V.; Zobov, N. F.; Polyansky, O. L. *J. Quantum Spectrosc. Radiat. Transfer* **2008**, *109*, 549.
- (114) Tarczay, G.; Császár, A. G.; Klopffer, W.; Szalay, V.; Allen, W. D.; Schaefer, H. F. *J. Chem. Phys.* **1999**, *110*, 11971.
- (115) Valeev, E. F.; Allen, W. D.; Schaefer, H. F., III; Császár, A. G. *J. Chem. Phys.* **2001**, *114*, 2875.
- (116) Brockway, L. O.; Bartell, L. S. *Rev. Sci. Instrum.* **1954**, *25*, 569.
- (117) Papoušek, D.; Aliev, M. R. *Molecular Vibrational-Rotational Spectra*; Elsevier: Amsterdam, 1982.
- (118) Verhoeven, J.; Dymanus, A. *J. Chem. Phys.* **1970**, *52*, 3222.
- (119) Császár, A. G.; Mills, I. M. *Spectrochim. Acta* **1997**, *53A*, 1101.
- (120) Richards, G. *Nature* **1979**, *278*, 507.
- (121) Schaefer, H. F. *Chimia* **1989**, *43*, 1.
- (122) Schaefer, H. F. *Science* **1986**, *231*, 1100.